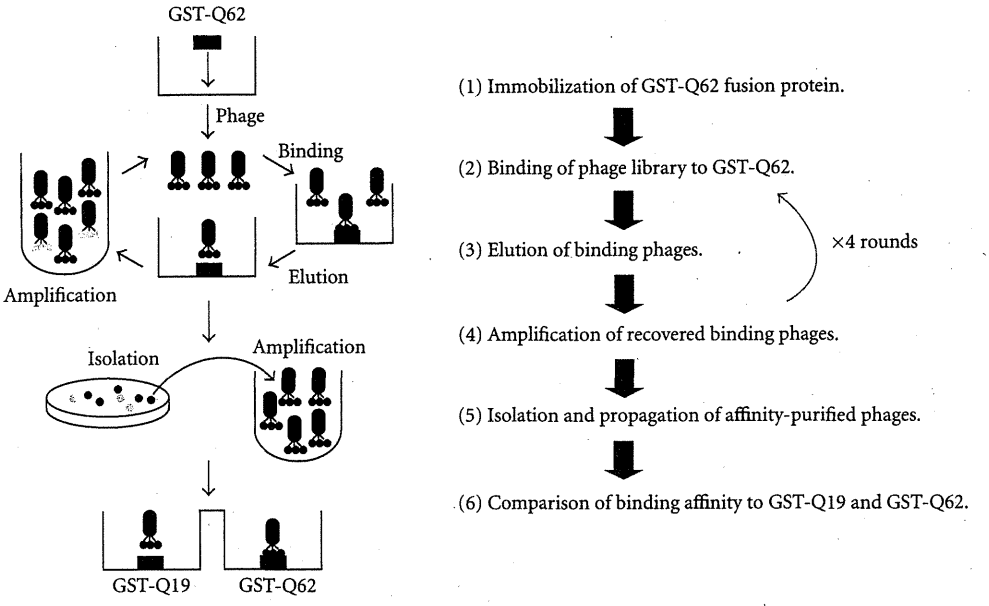

FIGURE 3: Phage display screening strategy for the identification of peptides that selectively bind to the expanded polyQ stretch. Phage libraries expressing random 11-amino acid sequences were first screened for their binding to GST-Q62 via 4 rounds of binding, elution, and amplification. Phage clones isolated from the first screening (350 clones) were further screened for their selective binding to pathologic length GST-Q62 compared to normal-length GST-Q19.

coincubated QBP1 with thio-Q62, and found that QBP1 dramatically inhibits thio-Q62 aggregation in a concentration-dependent manner, showing an almost complete inhibition at a stoichiometry of 3 : 1 (thio-Q62 : QBP1). A scrambled sequence of QBP1 (SCR; Trp-Pro-Ile-Trp-Ser-Lys-Gly-Asn-Asp-Trp-Phe) had no effect on thio-Q62 aggregation. Furthermore, addition of QBP1 after thio-Q62 aggregation has started resulted in inhibition of further aggregate formation, but it could not solubilize the aggregates already formed, suggesting that QBP1 inhibits the earlier stages in the aggregation process of the expanded polyQ protein [41].

4. Mechanism of Action of QBP1

To elucidate the molecular mechanisms by which QBP1 prevents aggregation of the expanded polyQ protein, we have characterized in detail the binding of QBP1 to the expanded polyQ stretch, and analyzed the effect of QBP1 on the conformation of the expanded polyQ protein. To characterize the binding specificities and affinities of QBP1 to the polyQ stretch, we employed the surface plasmon resonance (SPR) technique, which is a highly sensitive method for quantitatively measuring biomolecular interactions [42]. We found that QBP1 binds selectively to the thio-Q62 protein, with an equilibrium dissociation constant (K_d) of 5.7 μM, while it shows significant binding to neither thio-Q0 nor thio-Q19. These results clearly indicate the striking property of QBP1 to specifically recognize and bind to the expanded polyQ stretch, but not the normal length polyQ stretch. We also investigated the relationship between the polyQ binding affinities of QBP1 and its variants and their inhibitory effects on polyQ aggregation. We found a tight correlation between the binding affinities to the expanded polyQ stretch and inhibitory activities on polyQ aggregation of these peptides. Among these, $(QBP1)_2$, a tandem repeat of QBP1 exhibited the greatest binding affinity to thio-Q62 with a K_d value of 0.6 μM. We therefore conclude that binding affinity to the polyQ stretch is a critical determinant of the aggregation inhibitory activity.

Next, we analyzed the effect of QBP1 on the conformation of the expanded thio-polyQ protein [43]. Circular dichroism (CD) analyses revealed that QBP1 inhibits the conformational transition of the thio-Q62 protein to a β-sheet dominant structure. We further demonstrated for the first time that this β-sheet conformational transition of the expanded polyQ protein, which occurs at the level of the monomer before aggregation, causes cytotoxicity. Taken together, we conclude that QBP1 specifically binds to the expanded polyQ protein monomer and inhibits the toxic β-sheet conformational transition, and as a result, also inhibits the downstream aggregation and inclusion body formation (Figure 2).

5. The Therapeutic Effects of QBP1 Expression in Cell Culture Models of the PolyQ Diseases

We also determined whether QBP1 could exert therapeutic effects in cell culture models of the polyQ diseases [40]. Expanded polyQ proteins expressed in cultured cells have been shown to form inclusion bodies and cause cytotoxicity in a time- and polyQ length-dependent manner [44]. We first coexpressed QBP1 fused to cyan fluorescent protein (QBP1-CFP), with various-length polyQ proteins fused to yellow fluorescent protein (polyQ-YFP) in COS-7 cells, and examined

the effect of QBP1 on polyQ inclusion body formation and cytotoxicity. We found a prominent colocalization of QBP1-CFP with polyQ-YFP inclusions, indicating that QBP1 is capable of recognizing the polyQ stretches in cells. Notably, coexpression of QBP1-CFP significantly suppressed polyQ-YFP inclusion body formation, as well as cytotoxicity, and the inhibitory effects were stronger for shorter-length polyQ stretches (Q45 > Q57 > Q81). Furthermore, $(QBP1)_2$-CFP, which has a much higher affinity to the expanded polyQ stretch, exerted an even stronger inhibitory effect on polyQ inclusion body formation, consistent with our *in vitro* aggregation assay results [42].

The expanded polyQ protein is recently believed to form soluble oligomers before microscopically visible insoluble aggregates and inclusion bodies in cells, and these oligomers rather than aggregates or inclusion bodies have been suggested to cause cytotoxicity [24] (Figure 2). We therefore analyzed the effect of QBP1 on polyQ oligomer formation, by using fluorescence correlation spectroscopy (FCS), which is a highly sensitive technique for investigating the dynamics of fluorescent molecules at single molecule sensitivity [45]. We found that the time-dependent decrease in mobility and increase in size of the expanded polyQ-green fluorescent protein (polyQ-GFP) expressed in COS-7 cells, which indicates the formation of slowly moving oligomers, was significantly suppressed by the coexpression of $(QBP1)_2$-CFP [46]. Fluorescence resonance energy transfer (FRET) analyses also confirmed that $(QBP1)_2$ inhibits expanded polyQ oligomer formation in cultured cells [47]. These results are consistent with our *in vitro* observation that QBP1 inhibits the conformational transition of the polyQ protein monomer, which occurs before oligomer and aggregate formation.

6. Therapeutic Effects of QBP1 Expression in Animal Models of the PolyQ Diseases

From a therapeutic viewpoint, it is indispensable to demonstrate the therapeutic effect of QBP1 in *in vivo* disease models. We employed *Drosophila* models to elucidate the therapeutic effects of QBP1 expression on polyQ-induced neurodegeneration, since *Drosophila* models of the polyQ diseases are well established, easy to handle, and suitable for genetic analyses [48]. Transgenic flies expressing an expanded polyQ protein under an eye-specific promoter demonstrate accumulation of polyQ inclusion bodies and degeneration of the eyes. We crossed polyQ expressing flies and $(QBP1)_2$-CFP expressing flies, and found that coexpression of $(QBP1)_2$-CFP significantly suppresses eye degeneration, as well as inclusion body formation. We next examined the effect of $(QBP1)_2$-CFP coexpression on flies expressing the expanded polyQ protein under a panneuronal promoter, which causes premature death due to neurodegeneration. Notably, the median life span of polyQ expressing flies was dramatically improved from 5.5 days to 52 days by coexpression of $(QBP1)_2$-CFP, indicating that QBP1 successfully rescues premature death of the polyQ flies.

Table 2: Examples of protein transduction domains.

Name	Origin/design	Sequence
TAT	HIV-1 transactivator	Tyr-Gly-Arg-Lys-Lys-Arg-Arg-Gln-Arg-Arg-Arg
Antp	*Drosophila* Antennapedia	Arg-Gln-Ile-Lys-Ile-Trp-Phe-Gln-Asn-Arg-Arg-Met-Lys-Trp-Lys-Lys
VP22	HSV-1 structural protein	Asp-Ala-Ala-Thr-Ala-Thr-Arg-Gly-Arg-Ser-Ala-Ala-Ser-Arg-Pro-Thr-Glu-Arg-Pro-Arg-Ala-Pro-Ala-Arg-Ser-Ala-Ser-Arg-Pro-Arg-Arg-Pro-Val-Asp
Polyarginine	Synthetic	$(Arg)_n$
Transportan	Neuropeptide galanin + wasp peptide mastoparan	Gly-Trp-Thr-Leu-Asn-Ser-Ala-Gly-Tyr-Leu-Leu-Gly-Lys-Ile-Asn-Leu-Lys-Ala-Leu-Ala-Ala-Leu-Ala-Lys-Lys-Ile-Leu

These results clearly demonstrate the effectiveness of QBP1 on polyQ-induced neurodegeneration *in vivo*.

7. Therapeutic Effects of Protein Transduction Domain-Mediated Delivery of QBP1

To establish a therapy using QBP1, QBP1 needs to be delivered into affected neurons in the brain, rather than expressed by the crossing of genetically engineered animals. However, as QBP1 is an 11-amino acid peptide, it is too large to cross the cell membrane efficiently and enter cells on its own. To enable the efficient intracellular delivery of QBP1, we utilized protein transduction domains (PTDs), which are peptide sequences capable of penetrating the cell membrane and entering cells. These include the human immunodeficiency virus-1 TAT, *Drosophila* Antennapedia (Antp), herpes simplex virus-1 VP22, and the polyarginines (Table 2). PTDs have indeed been shown to efficiently deliver various biologically active molecules such as peptides, proteins, and nucleic acids into cells [49, 50].

We synthesized QBP1 peptides fused to the TAT or Antp PTD, and confirmed that both of them are efficiently transduced into cells upon addition to the medium of cultured cells, and inhibit inclusion body formation and cytotoxicity of the expanded polyQ protein [51]. To determine whether PTD-QBP1 administration is able to exert therapeutic effects on an *in vivo* model of the polyQ diseases, we first administered Antp-QBP1 to a *Drosophila* polyQ disease model, by adding the peptide into the culture food. Oral administration of Antp-QBP1 remarkably delayed premature death of the polyQ expressing flies compared with the control peptide Antp-SCR. In addition, flies administered with Antp-QBP1 had significantly fewer inclusion bodies compared to the control flies. These results indicated the potential of PTD-mediated delivery of QBP1 as a useful strategy to establish a molecular therapy using QBP1.

We next analyzed the therapeutic effect of Antp-QBP1 administration on a mouse model of the polyQ diseases [52]. Intraperitoneal injection of Antp-QBP1 resulted in a slight improvement of the weight loss in these mice, but did not improve the other phenotypes such as motor dysfunction and premature death. Furthermore, we could not detect a significant suppression of polyQ inclusion body formation by Antp-QBP1 administration in these mice. Although we confirmed the limited delivery of Antp-QBP1 into the mouse brain via intracerebroventricular and intrastriatal injection, we failed to detect a significant amount of Antp-QBP1 delivered in the brain via intraperitoneal injection. These results imply that Antp-QBP1 is unable to efficiently cross the blood-brain barrier (BBB) in mice, which is tighter than in flies.

8. Towards Designing Chemical Analogues of QBP1

Towards developing QBP1 as a therapeutic molecule for the polyQ diseases, we are taking another approach, which is designing low molecular weight chemical analogues of QBP1 with efficient BBB permeability. To design low molecular weight analogues of QBP1, we first determined the essential amino acids required for its activity and pharmacophores of QBP1.

We first synthesized various truncation mutants of QBP1, and tested their activities on polyQ aggregation. We found that truncation of Ser1 and Asn2, or truncation of Asp11 does not affect the inhibitory activity on polyQ aggregation whereas truncation of the N-terminal 4 amino acids (Ser1, Asn2, Trp3, and Lys4), or the C-terminal 2 amino acids (Phe10 and Asp11) results in dramatic loss of activity. These results imply that the aromatic amino acids (Trp3 and Phe10) are required for the activity of QBP1, and we therefore concluded that the central 8 amino acids (Trp-Lys-Trp-Trp-Pro-Gly-Ile-Phe) comprise the minimal active sequence of QBP1 [41]. Since other QBPs that we identified from the combinatorial screening also share Trp/Phe-rich sequences (Table 1), we next investigated the role of the Trp-Lys-Trp-Trp motif of QBP1 for its activity. Although the Trp-Lys-Trp-Trp motif alone is insufficient for inhibiting polyQ aggregation, a tandem repeat of Trp-Lys-Trp-Trp connected by an amino acid spacer was found to be as potent as the original QBP1, suggesting that the Trp-Lys-Trp-Trp motif plays an important role in recognizing the polyQ stretch.

We subsequently performed more comprehensive analyses on all amino acids within the QBP1 sequence by Ala scanning and D-amino acid scanning [53]. Substitutions of Ser1, Asn2, Lys4, Pro7, Gly8, or Asp11 to Ala did not show any significant effects on the activity of QBP1. On the other hand, Ala substitutions of Trp3, Trp5, Trp6, Ile9, or Phe10 led to a dramatic decrease in their activity on polyQ aggregation, indicating that the functional groups of these hydrophobic amino acids are essential for their inhibitory activity. Hence, the hydrophobic property of QBP1 may be important for its interaction with the expanded polyQ stretch. In addition, D-amino acid substitutions revealed that the internal amino acids (Trp3-Ile9) of QBP1 are sensitive to chirality inversion, which probably disrupts the active conformation of QBP1.

Another study using a series of peptide analogues of QBP1 elucidated the role of the Trp residues in the activity of QBP1 [54]. Although N-methylation at the main chain of Trp5 and Trp6, which would lose their potential as main chain hydrogen bond donors, resulted in a substantial loss of activity of QBP1, methylation of the indole nitrogen of these residues did not affect its activity, suggesting that the hydrogen bonding potential of the indole side chains are not necessary for the activity of QBP1.

In order to design chemical analogues of QBP1, it is also indispensable to obtain structural information on the mode of binding of QBP1 to the polyQ stretch. However, due to the high insolubility of the expanded polyQ protein, it has been a challenge to experimentally elucidate the structure of the polyQ stretch at atomic resolution in aqueous solution. Although a molecular dynamics study suggested hydrogen bonding between the amide groups of Ser1 to Gly8 of QBP1 and the main chain carbonyl groups of the polyQ stretch, and the role of the steric hindrance produced by Pro7 to prevent polyQ aggregation [55], there are some inconsistencies with the experimental results described above. Thus, further efforts to elucidate the detailed structure of the QBP1-polyQ complex would provide valuable information for designing chemical QBP1 analogues as a therapeutic molecule for the polyQ diseases.

9. Other Applications of QBP1

Since QBP1 is the only molecule which can distinguish between the expanded and normal length polyQ stretch, it is also useful for specific recognition of the expanded polyQ stretch. Indeed, we have confirmed the colocalization of QBP1 with polyQ inclusions [40], and recently, Raspe et al. also utilized QBP1-CFP to label expanded polyQ peptides within inclusion bodies in cultured cells [56]. These studies raise the possibility that QBP1 could also be developed as an *in vivo* imaging probe for detection of polyQ depositions in the brain.

Bauer et al. also employed QBP1 to recognize expanded polyQ proteins for their specific degradation by chaperone-mediated autophagy (CMA), in which Hsc70 recognizes and delivers substrate proteins to the lysosome for their degradation [57]. Coexpression of a modified QBP1, which was fused with Hsc70-binding motifs, with expanded polyQ proteins accelerated polyQ protein degradation, resulting in suppression of cytotoxicity in cultured cells. They further demonstrated that viral vector-mediated gene therapy of the modified QBP1 decreased polyQ protein aggregation and ameliorated phenotypes such as motor dysfunction and premature death in polyQ disease mice while viral expression of the original QBP1 alone also exhibited a modest therapeutic effect. These results clearly indicate the usefulness of QBP1 as a tool for specific recognition of the expanded polyQ protein.

10. Other Peptides/Proteins that Bind to PolyQ and Inhibit Aggregation

Discovery of QBP1 has facilitated research towards applying various polyQ-binding molecules such as peptides and proteins to prevent misfolding and aggregation of the expanded polyQ protein like as QBP1. Kazantsev et al. designed a bivalent peptide comprised of two normal-length polyQ stretches connected by a spacer, which is expected to bind to the expanded polyQ stretch, and showed that expression of this peptide suppresses polyQ inclusion body formation and cytotoxicity in cell culture and *Drosophila* polyQ disease models [58]. We also designed a normal-length polyQ stretch with a Pro insertion, which disrupts the ordered structure of the polyQ stretch, and showed that this peptide successfully delays polyQ aggregation *in vitro* [59]. However, since these rationally designed peptides contain short polyQ stretches that can be recruited to expanded polyQ aggregates, they have the risk of accelerating polyQ aggregation and enhancing toxicity under certain conditions. Furthermore, the therapeutic effects of these peptides were much weaker compared to QBP1, which is the optimal peptide sequence identified by a combinatorial screening approach for its specific binding affinity to the expanded polyQ stretch, and is the only molecule that has been shown to inhibit the toxic β-sheet conformational transition of the expanded polyQ protein [43].

Several intracellular antibodies, known as intrabodies, which bind to the expanded polyQ protein and inhibit its aggregation have also been identified to date. In 2001, Lecerf et al. identified the intrabody C4 that binds to the N-terminus of huntingtin (htt), the disease-causing protein of Huntington's disease (HD), by phage display library screening [60]. Subsequently, they and other groups further showed that expression of C4 as well as other intrabodies, namely, MW7, V_L12.3, Happ1, and EM48, all of which bind to the polyQ adjacent regions in htt, leads to suppression of htt aggregation and neurodegeneration in cell culture, *Drosophila*, and mouse models of HD [60–67]. The use of intrabodies is an attractive therapeutic approach with regard to their high binding affinity to the disease-causing proteins. However, since the intrabodies identified so far recognize a region in htt other than the polyQ stretch itself, they cannot be applied for the other polyQ diseases, and may cause unfavorable side effects by binding to the wild type htt with a normal polyQ stretch.

11. Perspectives

In this review, we introduced our therapeutic strategy against the polyQ neurodegenerative diseases using QBP1, a peptide sequence that specifically recognizes the expanded polyQ stretch, which we identified from phage display screening. Although we have provided convincing evidence on the potential of QBP1 as a therapy for the polyQ diseases, by demonstrating its ability to inhibit misfolding and aggregation, resulting in suppression of polyQ-induced neurodegeneration *in vivo*, the major problem we are currently facing is its delivery into the brain. Although viral vector-mediated gene therapy may have potential for the delivery of QBP1 into the brain, the difficulty in controlling gene expression, toxicity, and limited delivery within the brain discourage this approach. The success of PTD-mediated delivery of QBP1 and its therapeutic effects in a *Drosophila* model of the polyQ diseases have shed light on the potential of PTDs for *in vivo* delivery of QBP1. Recently, an unconventional secretion signal overlapped with the Antp sequence was identified, which enables secretion from cells in addition to entry into cells via Antp [68], suggesting the potential of identifying or designing novel PTDs with high BBB permeability. Since most therapeutic molecules currently in clinical use are chemical compounds, we believe the most promising approach is to design low molecular weight chemical QBP1 analogues with efficient BBB permeability. Further clarification of the mode of binding of QBP1 to the expanded polyQ stretch and detailed structural analyses of the QBP1-polyQ complex will facilitate the designing of chemical analogues of QBP1 as a potential therapeutic molecule for the polyQ diseases.

Although our work has been focused on the polyQ diseases, our approach could also be applied for a broad range of other neurodegenerative diseases including Alzheimer's disease and Parkinson's disease, which are caused by a common mechanism based on protein misfolding and aggregation. Indeed, various peptides/proteins that inhibit protein aggregation have been reported to exert therapeutic effects in cell culture and animal models of these diseases [69, 70]. We hope that in the near future, aggregation inhibitor peptide-based drugs against protein misfolding neurodegenerative diseases will be developed and bring a cure to patients suffering from these currently intractable neurodegenerative diseases.

Acknowledgments

The authors thank Nobuhiro Fujikake, Takashi Inui, Hironobu Naiki, Yuji Goto, Yasuo Takahashi, Masataka Kinjo, and Osamu Onodera for their helpful discussions, and Yuma Okamoto, Chiyomi Ito, Reiko Sasaki, and Hirokazu Matsushima for their technical assistance. The authors' work on the polyglutamine diseases is supported in part by Grants-in-Aid for Scientific Research on Priority Areas (Advanced Brain Science Project, Research on Pathomechanisms of Brain Disorders, Life of Proteins, Protein Community, Water and Biomolecules, Transportsome, and Intracellular Proteolysis to Y. Nagai), and on Innovative Areas (Synapse and Neurocircuit Pathology to Y. Nagai; Amyloid Propagation to H. A. Popiel) from the Ministry of Education, Culture, Sports, Science, and Technology, Japan; by Grants-in-Aid for Scientific Research (B), (C), and Challenging Exploratory Research (to Y. Nagai), for Young Scientists (B; to H. A. Popiel), and a JSPS Postdoctoral Fellowship for Foreign Researchers (to H. A. Popiel), from the Japan Society for the Promotion of Science, Japan; by a Grant-in-Aid for the Research Committee for Ataxic Diseases (to Y. Nagai) from the Ministry of Health, Labor, and Welfare, Japan; by a grant from Core Research for Evolutional Science and Technology (CREST) of the Japan Science and Technology Agency (to

Y. Nagai); by grants from Takeda Science Foundation, Naito Foundation, AstraZeneca (to Y. Nagai); by a Scholarship for Foreign Nationals in Japan from Ichiro Kanehara Foundation (to H. A. Popiel).

References

[1] J. P. Taylor, J. Hardy, and K. H. Fischbeck, "Toxic proteins in neurodegenerative disease," *Science*, vol. 296, no. 5575, pp. 1991–1995, 2002.

[2] C. Soto, "Unfolding the role of protein misfolding in neurodegenerative diseases," *Nature Reviews Neuroscience*, vol. 4, no. 1, pp. 49–60, 2003.

[3] C. A. Ross and M. A. Poirier, "What is the role of protein aggregation in neurodegeneration," *Nature Reviews Molecular Cell Biology*, vol. 6, no. 11, pp. 891–898, 2005.

[4] J. F. Gusella and M. E. MacDonald, "Molecular genetics: unmasking polyglutamine triggers in neurodegenerative disease," *Nature Reviews Neuroscience*, vol. 1, no. 2, pp. 109–115, 2000.

[5] H. T. Orr and H. Y. Zoghbi, "Trinucleotide repeat disorders," *Annual Review of Neuroscience*, vol. 30, pp. 575–621, 2007.

[6] A. R. La Spada, E. M. Wilson, D. B. Lubahn, A. E. Harding, and K. H. Fischbeck, "Androgen receptor gene mutations in X-linked spinal and bulbar muscular atrophy," *Nature*, vol. 352, no. 6330, pp. 77–79, 1991.

[7] E. Marcy, M. Christine, P. Mabel et al., "A novel gene containing a trinucleotide repeat that is expanded and unstable on Huntington's disease chromosomes," *Cell*, vol. 72, no. 6, pp. 971–983, 1993.

[8] H. T. Orr, M. Y. Chung, S. Banfi et al., "Expansion of an unstable trinucleotide CAG repeat in spinocerebellar ataxia type 1," *Nature Genetics*, vol. 4, no. 3, pp. 221–226, 1993.

[9] G. Imbert, F. Saudou, G. Yvert et al., "Cloning of the gene for spinooerebellar ataxia 2 reveals a locus with high sensitivity to expanded CAG/glutamine repeats," *Nature Genetics*, vol. 14, no. 3, pp. 285–291, 1996.

[10] S. M. Pulst, A. Nechiporuk, T. Nechiporuk et al., "Moderate expansion of a normally biallelic trinucleotide repeat in spinooerebellar ataxia type 2," *Nature Genetics*, vol. 14, no. 3, pp. 269–276, 1996.

[11] K. Sanpei, H. Takano, S. Igarashi et al., "Identification of the spinocerebellar ataxia type 2 gene using a direct identification of repeat expansion and cloning technique, direct," *Nature Genetics*, vol. 14, no. 3, pp. 277–284, 1996.

[12] Y. Kawaguchi, T. Okamoto, M. Taniwaki et al., "CAG expansions in a novel gene for Machado-Joseph disease at chromosome 14q32.1," *Nature Genetics*, vol. 8, no. 3, pp. 221–228, 1994.

[13] O. Zhuchenko, J. Bailey, P. Bonnen et al., "Autosomal dominant cerebellar ataxia (SCA6) associated with small polyglutamine expansions in the α_{1A}-voltage-dependent calcium channel," *Nature Genetics*, vol. 15, no. 1, pp. 62–69, 1997.

[14] G. David, N. Abbas, G. Stevanin et al., "Cloning of the SCA7 gene reveals a highly unstable CAG repeat expansion," *Nature Genetics*, vol. 17, no. 1, pp. 65–70, 1997.

[15] K. Nakamura, S. Y. Jeong, T. Uchihara et al., "SCA17, a novel autosomal dominant cerebellar ataxia caused by an expanded polyglutamine in TATA-binding protein," *Human Molecular Genetics*, vol. 10, no. 14, pp. 1441–1448, 2001.

[16] R. Koide, T. Ikeuchi, O. Onodera et al., "Unstable expansion of CAG repeat in hereditary dentatorubral- pallidoluysian atrophy (DRPLA)," *Nature Genetics*, vol. 6, no. 1, pp. 9–13, 1994.

[17] S. Nagafuchi, H. Yanagisawa, K. Sato et al., "Dentatorubral and pallidoluysian atrophy expansion of an unstable CAG trinucleotide on chromosome 12p," *Nature Genetics*, vol. 6, no. 1, pp. 14–18, 1994.

[18] L. Mangiarini, K. Sathasivam, M. Seller et al., "Exon I of the HD gene with an expanded CAG repeat is sufficient to cause a progressive neurological phenotype in transgenic mice," *Cell*, vol. 87, no. 3, pp. 493–506, 1996.

[19] J. M. Warrick, H. L. Paulson, G. L. Gray-Board et al., "Expanded polyglutamine protein forms nuclear inclusions and causes neural degeneration in Drosophila," *Cell*, vol. 93, no. 6, pp. 939–949, 1998.

[20] P. W. Faber, J. R. Alter, M. E. Macdonald, and A. C. Hart, "Polyglutamine-mediated dysfunction and apoptotic death of a *Caenorhabditis elegans* sensory neuron," *Proceedings of the National Academy of Sciences of the United States of America*, vol. 96, no. 1, pp. 179–184, 1999.

[21] J. M. Ordway, S. Tallaksen-Greene, C. A. Gutekunst et al., "Ectopically expressed CAG repeats cause intranuclear inclusions and a progressive late onset neurological phenotype in the mouse," *Cell*, vol. 91, no. 6, pp. 753–763, 1997.

[22] A. Michalik and C. Van Broeckhoven, "Pathogenesis of polyglutamine disorders: aggregation revisited," *Human Molecular Genetics*, vol. 12, no. 2, pp. R173–R186, 2003.

[23] J. Shao and M. I. Diamond, "Polyglutamine diseases: emerging concepts in pathogenesis and therapy," *Human Molecular Genetics*, vol. 16, no. R2, pp. R115–R123, 2007.

[24] Y. Nagai and H. A. Popiel, "Conformational changes and aggregation of expanded polyglutamine proteins as therapeutic targets of the polyglutamine diseases: exposed β-sheet hypothesis," *Current Pharmaceutical Design*, vol. 14, no. 30, pp. 3267–3279, 2008.

[25] P. O. Bauer and N. Nukina, "The pathogenic mechanisms of polyglutamine diseases and current therapeutic strategies," *Journal of Neurochemistry*, vol. 110, no. 6, pp. 1737–1765, 2009.

[26] A. J. Williams and H. L. Paulson, "Polyglutamine neurodegeneration: protein misfolding revisited," *Trends in Neurosciences*, vol. 31, no. 10, pp. 521–528, 2008.

[27] T. Shimohata, T. Nakajima, M. Yamada et al., "Expanded polyglutamine stretches interact with TAF(II)130, interfering with CREB-dependent transcription," *Nature Genetics*, vol. 26, no. 1, pp. 29–36, 2000.

[28] F. C. Nucifora, M. Sasaki, M. F. Peters et al., "Interference by huntingtin and atrophin-1 with CBP-mediated transcription leading to cellular toxicity," *Science*, vol. 291, no. 5512, pp. 2423–2428, 2001.

[29] C. J. Cummings, M. A. Mancini, B. Antalffy, D. B. DeFranco, H. T. Orr, and H. Y. Zoghbi, "Chaperone suppression of aggregation and altered subcellular proteasome localization imply protein misfolding in SCA1," *Nature Genetics*, vol. 19, no. 2, pp. 148–154, 1998.

[30] Y. Chai, S. L. Koppenhafer, N. M. Bonini, and H. L. Paulson, "Analysis of the role of heat shock protein (Hsp) molecular chaperones in polyglutamine disease," *Journal of Neuroscience*, vol. 19, no. 23, pp. 10338–10347, 1999.

[31] Y. Nagai, O. Onodera, J. Chun, W. J. Strittmatter, and J. R. Burke, "Expanded polyglutamine domain proteins bind neurofilament and alter the neurofilament network," *Experimental Neurology*, vol. 155, no. 2, pp. 195–203, 1999.

[32] N. A. Di Prospero and K. H. Fischbeck, "Therapeutics development for triplet repeat expansion diseases," *Nature Reviews Genetics*, vol. 6, no. 10, pp. 756–765, 2005.

[33] J. S. Steffan, L. Bodai, J. Pallos et al., "Histone deacetylase inhibitors arrest polyglutamine-dependent neurodegeneration in *Drosophila*," *Nature*, vol. 413, no. 6857, pp. 739–743, 2001.

[34] N. F. Bence, R. M. Sampat, and R. R. Kopito, "Impairment of the ubiquitin-proteasome system by protein aggregation," *Science*, vol. 292, no. 5521, pp. 1552–1555, 2001.

[35] S. Gunawardena, L. S. Her, R. G. Brusch et al., "Disruption of axonal transport by loss of huntingtin or expression of pathogenic polyQ proteins in *Drosophila*," *Neuron*, vol. 40, no. 1, pp. 25–40, 2003.

[36] G. Szebenyi, G. A. Morfini, A. Babcock et al., "Neuropathogenic forms of huntingtin and androgen receptor inhibit fast axonal transport," *Neuron*, vol. 40, no. 1, pp. 41–52, 2003.

[37] G. Bates, "Huntingtin aggregation and toxicity in Huntington's disease," *Lancet*, vol. 361, no. 9369, pp. 1642–1644, 2003.

[38] M. Herbst and E. E. Wanker, "Therapeutic approaches to polyglutamine diseases: combating protein misfolding and aggregation," *Current Pharmaceutical Design*, vol. 12, no. 20, pp. 2543–2555, 2006.

[39] Y. Trottier, Y. Lutz, G. Stevanin et al., "Polyglutamine expansion as a pathological epitope in Huntington's disease and four dominant cerebellar ataxias," *Nature*, vol. 378, no. 6555, pp. 403–406, 1995.

[40] Y. Nagai, T. Tucker, H. Ren et al., "Inhibition of polyglutamine protein aggregation and cell death by novel peptides identified by phage display screening," *Journal of Biological Chemistry*, vol. 275, no. 14, pp. 10437–10442, 2000.

[41] H. Ren, Y. Nagai, T. Tucker, W. J. Strittmatter, and J. R. Burke, "Amino acid sequence requirements of Peptides that inhibit polyglutamine-protein aggregation and cell death," *Biochemical and Biophysical Research Communications*, vol. 288, no. 3, pp. 703–710, 2001.

[42] Y. Okamoto, Y. Nagai, N. Fujikake et al., "Surface plasmon resonance characterization of specific binding of polyglutamine aggregation inhibitors to the expanded polyglutamine stretch," *Biochemical and Biophysical Research Communications*, vol. 378, no. 3, pp. 634–639, 2009.

[43] Y. Nagai, T. Inui, H. A. Popiel et al., "A toxic monomeric conformer of the polyglutamine protein," *Nature Structural and Molecular Biology*, vol. 14, no. 4, pp. 332–340, 2007.

[44] O. Onodera, J. R. Burke, S. E. Miller et al., "Oligomerization of expanded-polyglutamine domain fluorescent fusion proteins in cultured mammalian cells," *Biochemical and Biophysical Research Communications*, vol. 238, no. 2, pp. 599–605, 1997.

[45] M. Eigen and R. Rigler, "Sorting single molecules: application to diagnostics and evolutionary biotechnology," *Proceedings of the National Academy of Sciences of the United States of America*, vol. 91, no. 13, pp. 5740–5747, 1994.

[46] Y. Takahashi, Y. Okamoto, H. A. Popiel et al., "Detection of polyglutamine protein oligomers in cells by fluorescence correlation spectroscopy," *Journal of Biological Chemistry*, vol. 282, no. 33, pp. 24039–24048, 2007.

[47] T. Takahashi, S. Kikuchi, S. Katada, Y. Nagai, M. Nishizawa, and O. Onodera, "Soluble polyglutamine oligomers formed prior to inclusion body formation are cytotoxic," *Human Molecular Genetics*, vol. 17, no. 3, pp. 345–356, 2008.

[48] Y. Nagai, N. Fujikake, K. Ohno et al., "Prevention of polyglutamine oligomerization and neurodegeneration by the peptide inhibitor QBP1 in *Drosophila*," *Human Molecular Genetics*, vol. 12, no. 11, pp. 1253–1259, 2003.

[49] A. Joliot and A. Prochiantz, "Transduction peptides: from technology to physiology," *Nature Cell Biology*, vol. 6, no. 3, pp. 189–196, 2004.

[50] J. S. Wadia and S. F. Dowdy, "Protein transduction technology," *Current Opinion in Biotechnology*, vol. 13, no. 1, pp. 152–156, 2002.

[51] H. A. Popiel, Y. Nagai, N. Fujikake, and T. Toda, "Protein transduction domain-mediated delivery of QBP1 suppresses polyglutamine-induced neurodegeneration *in vivo*," *Molecular Therapy*, vol. 15, no. 2, pp. 303–309, 2007.

[52] H. A. Popiel, Y. Nagai, N. Fujikake, and T. Toda, "Delivery of the aggregate inhibitor peptide QBP1 into the mouse brain using PTDs and its therapeutic effect on polyglutamine disease mice," *Neuroscience Letters*, vol. 449, no. 2, pp. 87–92, 2009.

[53] K. Tomita, H. A. Popiel, Y. Nagai et al., "Structure-activity relationship study on polyglutamine binding peptide QBP1," *Bioorganic and Medicinal Chemistry*, vol. 17, no. 3, pp. 1259–1263, 2009.

[54] L. Hamuro, G. Zhang, T. J. Tucker, C. Self, W. J. Strittmatter, and J. R. Burke, "Optimization of a polyglutamine aggregation inhibitor peptide (QBP1) using a thioflavin T fluorescence assay," *Assay and Drug Development Technologies*, vol. 5, no. 5, pp. 629–636, 2007.

[55] R. S. Armen, B. M. Bernard, R. Day, D. O. Alonso, and V. Daggett, "Characterization of a possible amyloidogenic precursor in glutamine-repeat neurodegenerative diseases," *Proceedings of the National Academy of Sciences of the United States of America*, vol. 102, no. 38, pp. 13433–13438, 2005.

[56] M. Raspe, J. Gillis, H. Krol et al., "Mimicking proteasomal release of polyglutamine peptides initiates aggregation and toxicity," *Journal of Cell Science*, vol. 122, no. 18, pp. 3262–3271, 2009.

[57] P. O. Bauer, A. Goswami, H. K. Wong et al., "Harnessing chaperone-mediated autophagy for the selective degradation of mutant huntingtin protein," *Nature Biotechnology*, vol. 28, no. 3, pp. 256–263, 2010.

[58] A. Kazantsev, H. A. Walker, N. Slepko et al., "A bivalent Huntingtin binding peptide suppresses polyglutamine aggregation and pathogenesis in *Drosophila*," *Nature Genetics*, vol. 30, no. 4, pp. 367–376, 2002.

[59] H. A. Popiel, Y. Nagai, O. Onodera et al., "Disruption of the toxic conformation of the expanded polyglutamine stretch leads to suppression of aggregate formation and cytotoxicity," *Biochemical and Biophysical Research Communications*, vol. 317, no. 4, pp. 1200–1206, 2004.

[60] J. M. Lecerf, T. L. Shirley, Q. Zhu et al., "Human single-chain Fv intrabodies counteract *in situ* huntingtin aggregation in cellular models of Huntington's disease," *Proceedings of the National Academy of Sciences of the United States of America*, vol. 98, no. 8, pp. 4764–4769, 2001.

[61] W. J. Wolfgang, T. W. Miller, J. M. Webster et al., "Suppression of Huntington's disease pathology in *Drosophila* by human single-chain Fv antibodies," *Proceedings of the National Academy of Sciences of the United States of America*, vol. 102, no. 32, pp. 11563–11568, 2005.

[62] A. Snyder-Keller, J. A. McLear, T. Hathorn, and A. Messer, "Early or late-stage anti-N-terminal huntingtin intrabody gene therapy reduces pathological features in B6.HDR6/1 mice," *Journal of Neuropathology and Experimental Neurology*, vol. 69, no. 10, pp. 1078–1085, 2010.

[63] A. Khoshnan, J. Ko, and P. H. Patterson, "Effects of intracellular expression of anti-huntingtin antibodies of various specificities on mutant huntingtin aggregation and toxicity," *Proceedings of the National Academy of Sciences of the United States of America*, vol. 99, no. 2, pp. 1002–1007, 2002.

[64] D. W. Colby, Y. Chu, J. P. Cassady et al., "Potent inhibition of huntingtin aggregation and cytotoxicity by a disulfide bond-free single-domain intracellular antibody," *Proceedings of the National Academy of Sciences of the United States of America*, vol. 101, no. 51, pp. 17616–17621, 2004.

[65] A. L. Southwell, A. Khoshnan, D. E. Dunn, C. W. Bugg, D. C. Lo, and P. H. Patterson, "Intrabodies binding the proline-rich domains of mutant Huntingtin increase its turnover and reduce neurotoxicity," *Journal of Neuroscience*, vol. 28, no. 36, pp. 9013–9020, 2008.

[66] A. L. Southwell, J. Ko, and P. H. Patterson, "Intrabody gene therapy ameliorates motor, cognitive, and neuropathological symptoms in multiple mouse models of Huntington's disease," *Journal of Neuroscience*, vol. 29, no. 43, pp. 13589–13602, 2009.

[67] C. E. Wang, H. Zhou, J. R. McGuire et al., "Suppression of neuropil aggregates and neurological symptoms by an intracellular antibody implicates the cytoplasmic toxicity of mutant huntingtin," *Journal of Cell Biology*, vol. 181, no. 5, pp. 803–816, 2008.

[68] E. Dupont, A. Prochiantz, and A. Joliot, "Identification of a signal peptide for unconventional secretion," *Journal of Biological Chemistry*, vol. 282, no. 12, pp. 8994–9000, 2007.

[69] A. M. Bodles, O. M. El-Agnaf, B. Greer, D. J. Guthrie, and G. B. Irvine, "Inhibition of fibril formation and toxicity of a fragment of α-synuclein by an N-methylated peptide analogue," *Neuroscience Letters*, vol. 359, no. 1-2, pp. 89–93, 2004.

[70] C. Soto, E. M. Sigurdsson, L. Morelli, R. A. Kumar, E. M. Castaño, and B. Frangione, "β-sheet breaker peptides inhibit fibrillogenesis in a rat brain model of amyloidosis: implications for Alzheimer's therapy," *Nature Medicine*, vol. 4, no. 7, pp. 822–826, 1998.

Human Molecular Genetics, 2011, Vol. 20, No. 15 **2975–2983**
doi:10.1093/hmg/ddr201
Advance Access published on May 24, 2011

Endoplasmic reticulum stress response in P104L mutant caveolin-3 transgenic mice

Atsushi Kuga[1,2], Yutaka Ohsawa[2], Tadashi Okada[2], Fumio Kanda[1], Motoi Kanagawa[1], Tatsushi Toda[1] and Yoshihide Sunada[2,*]

[1]Division of Neurology/Molecular Brain Science, Kobe University Graduate School of Medicine, 7-5-1 Kusunoki-cho, Kobe, Hyogo 650-0017, Japan and [2]Department of Neurology, Kawasaki Medical School, 577 Matsushima, Kurashiki, Okayama 701-0192, Japan

Received March 28, 2011; Revised March 28, 2011; Accepted April 28, 2011

Mutations in the caveolin-3 gene cause autosomal dominant limb-girdle muscular dystrophy 1C (LGMD1C). However, the precise molecular pathogenesis of caveolin-3-related muscular dystrophy remains uncertain. Here, we demonstrate the effect of gene dosage on the severity of the myopathic phenotype in P104L mutant caveolin-3 (mCav3^{P104L}) transgenic mice, a model of LGMD1C. We analyzed the endoplasmic reticulum (ER) stress response in the transgenic mice and found upregulated transcription of the molecular chaperone, glucose-regulated protein (GRP78). Moreover, signaling downstream of GRP78 in the myofibers was activated toward apoptosis. However, terminal transferase dUTP nick end labeling assays detected a few apoptotic nuclei in transgenic mouse skeletal muscle, probably due to the transcriptional activation of Dad1, an anti-apoptotic factor in the ER. These findings suggest that the ER stress response caused by mCav3^{P104L} plays a role in the pathogenesis of LGMD1C as a toxic gain of function effect.

INTRODUCTION

Caveolae are characterized as flask-shaped invaginations of the plasma membrane (1). Caveolin is a major structural component of caveolae (2) and it also functions as a scaffolding protein to concentrate and regulate many classes of signaling molecules. Distinct genes encode the isoforms, caveolin-1, -2 and -3. Caveolin-3 is specifically expressed in muscle cells (3). Co-expressed caveolins-1 and -2 form hetero-oligomers in non-muscle cells, whereas caveolin-3 forms homo-oligomers in muscle cells. Different mutations in the human caveolin-3 gene have been associated with several muscle diseases that are collectively called caveolinopathies and include limb-girdle muscular dystrophy, distal myopathy and rippling muscle disease (4,5). A mutant caveolin-3 with a single amino acid substitution from proline to leucine at amino acid residue 104 (mCav3^{P104L}) was originally identified from a genetic analysis of autosomal dominant limb-girdle muscular dystrophy 1C (LGMD1C) (6).

Since LGMD1C is inherited as an autosomal dominant trait, mCav3^{P104L} presumably has a dominant-negative effect on the molecular pathogenesis of caveolinopathy. Studies *in vitro* have shown that homo-oligomers of wild-type caveolin-3 translocate to the cell membrane via the endoplasmic reticulum (ER)–Golgi network, whereas mCav3^{P104L} does not target the cell membrane (7). The hetero-oligomers formed between wild-type caveolin-3 and mCav3^{P104L} in the ER–Golgi system are degraded by the ubiquitin–proteasome proteolytic pathway, which might lead to the loss of caveolin-3 in LGMD1C (7,8). Targeted downregulation of caveolin-3 gene in differentiating C2C12 myoblasts can inhibit myotube formation (9). Expression of mCav3^{P104L} can trigger a loss of caveolin-3 during C2C12 cell differentiation (10). These results suggest that the secondary loss of caveolin-3 due to mCav3^{P104L} is associated with the molecular pathology of LGMD1C. However, whether mCav3^{P104L} has a gain of function effect that contributes to the pathogenesis of LGMD1C remains uncertain.

The ER stress response to the accumulation of a mutant protein has recently garnered interest among those investigating the pathogenesis of neurodegenerative disorders. For instance, the cytoplasmic aggregation of alpha-synuclein that is a pathological hallmark of Parkinson's disease is accelerated in a form of familial Parkinson's disease caused by a dominant mutation of the alpha-synuclein gene (11). In addition, several genes responsible for autosomal recessive Parkinson's disease

*To whom correspondence should be addressed. Tel: +81 864621111; Fax: +81 864621199; Email: ysunada@med.kawasaki-m.ac.jp

are involved in the ER-associated ubiquitination system (12). However, the ER stress response has not been intensively studied from the viewpoint of muscular dystrophy. We previously generated and studied mCav3^{P104L} transgenic mice as a model of LGMD1C (13–15). The present study investigates the ER stress response in mCav3^{P104L} transgenic mice as well as a possible gain of function effect of mCav3^{P104L}.

RESULTS

Dose effect of mCav3^{P104L} transgene on the severity of the myopathic phenotype

We previously identified a severe myopathic phenotype in mCav3^{P104L} hemizygous transgenic mice (13). Homozygous mCav3^{P104L} mice were obtained by hemizygous intercrossing and southern blot analysis confirmed the wild-type, hemizygous and homozygous transgenic mouse genotypes (Fig. 1A). Western blot analysis detected less caveolin-3 protein in hemizygous than in homozygous mice (Fig. 1B). We then analyzed the effect of mCav3^{P104L} gene dosages on the myopathic phenotype. Consistent with our previous findings (13), hemizygous mice weighed less than wild-type mice, but the difference did not reach statistical significance. The difference in body weight between homozygous and wild-type mice was statistically confirmed from 4 and 12 weeks of age at all measured points (Fig. 1C). We also found that grip strength significantly differed between the groups from 4 and 12 weeks of age at most measured points (Fig. 1D). Central nucleation or mononuclear infiltration was essentially absent. We measured average areas of myofibers in quadriceps muscles from mice of each genotype (Fig. 1E). Small myofibers were more frequent in the order of homozygous > hemizygous > wild-type mice and non-parametrical statistical analysis confirmed significant differences among the groups (Fig. 1F). The frequency of small myofibers in the gastrocnemius muscle also significantly differed among the genotypes (Supplementary Material, Fig. S1A and B). These data showed that the dose of the mCav3^{P104L} transgene correlated with the severity of the myopathic phenotype.

Residual level of caveolin-3 protein and the myopathic phenotype

The residual amount of caveolin-3 protein in mCav3^{P104L} transgenic mice was <20% of that in wild-type mice (Fig. 1B). To confirm whether other caveolin isoforms counteract the loss of caveolin-3 in muscle cells, we analyzed the expression of caveolin-1 and -2 in mCav3^{P104L} transgenic mice. Messenger RNA levels of caveolin-1 and -2 were increased about 1.5-fold in the skeletal muscle of homozygous mice, whereas no significant change was detectable in hemizygous mice (Fig. 2A and B). Western blotting showed that these changes were consistent at the protein level (Fig. 2C and D). However, immunohistochemistry revealed that upregulated caveolins-1 and -2 were not localized to the sarcolemma, but to the muscle interstitial region containing blood vessels (Fig. 2E). These results indicated that caveolin-1 and -2 upregulation does not compensate for the lack of caveolin-3 function in skeletal muscle. Interestingly, less caveolin-3 protein was detected in hemizygous than in homozygous mice (Fig. 1B). Since the antibodies used for western blotting cannot distinguish between endogenous and mutant caveolin-3 protein, these results suggest that the increased amount of residual mCav3^{P104L} protein in homozygous mice led to more severe myopathy via a toxic gain of function effect.

Localization of mCav3^{P104L} protein and ER stress response

We investigated the subcellular localization of mCav3^{P104L} *in vitro*. Cosmids containing a fluorescent marker for the ER (DsRed-KDEL) or for the Golgi complex (DsRed-Golgi) were cotransfected with wild-type caveolin-3 or mCav3^{P104L} into C2C12 myoblasts. Immunostaining showed surface membrane localization of wild-type caveolin-3, whereas mCAV3^{P104L} did not target the surface membrane and tended to colocalize with the Golgi, but not the ER marker (Fig. 3). The Golgi marker and mCAV3^{P104L} also colocalized in COS7 cells (Supplementary Material, Fig. S2).

We investigated whether mCav3^{P104L} in muscle cells could induce the ER stress response in mCav3^{P104L} transgenic mice by analyzing the expression of genes related to ER stress. Messenger RNA levels of glucose-regulated protein (GRP78), a molecular chaperone in the ER (16), increased 1.5- and 2.5-fold in hemizygous and homozygous mice, respectively, compared with wild-type mice (Fig. 4A and C). Western blotting also confirmed GRP78 induction at the protein level (Fig. 4B and D). Eukaryotic initiation factor 2α (eIF2α) is phosphorylated in response to GRP78 induction under ER stress (17,18). Although the total amount of eIF2α did not significantly change, the amount of phosphorylated eIF2α was increased in transgenic compared with wild-type mice (Fig. 4B and E). We then evaluated the mRNA levels of C/EBP homologous protein (CHOP), which is a pre-apoptotic transcription factor that functions downstream of phosphorylated eIF2α (18,19), and found that they were significantly increased in mCav3^{P104L} transgenic mice (Fig. 4A and C). Overall, these results suggested that mCav3^{P104L} accumulates in the Golgi complex and induces the ER stress response mediated by the molecular chaperone GRP78 and its downstream pathway.

ER stress response toward apoptosis in myofibers from mCav3^{P104L} transgenic mice

We compared the consequences of the mCav3^{P104L}-induced ER stress response using terminal transferase dUTP nick end labeling (TUNEL) assays of quadriceps muscles from mCav3^{P104L} transgenic mice and other mouse models of muscular dystrophy, namely *mdx* and *dy* mice (Fig. 5A). Several TUNEL-positive nuclei of interstitial cells were located outside the myofibers of *mdx* mice and *dy* mice. To distinguish these cells from apoptotic myofibers, we counted the number of myofibers with TUNEL-positive nuclei. Unlike *mdx* mice and *dy* mice, TUNEL-positive nuclei in mCav3^{P104L} transgenic mice were mainly located inside myofibers. Although the average number of TUNEL-positive myofibers was increased in mCav3^{P104L} transgenic mice, the increase was modest compared with the amount in *mdx* mice and *dy* mice (Fig. 5B).

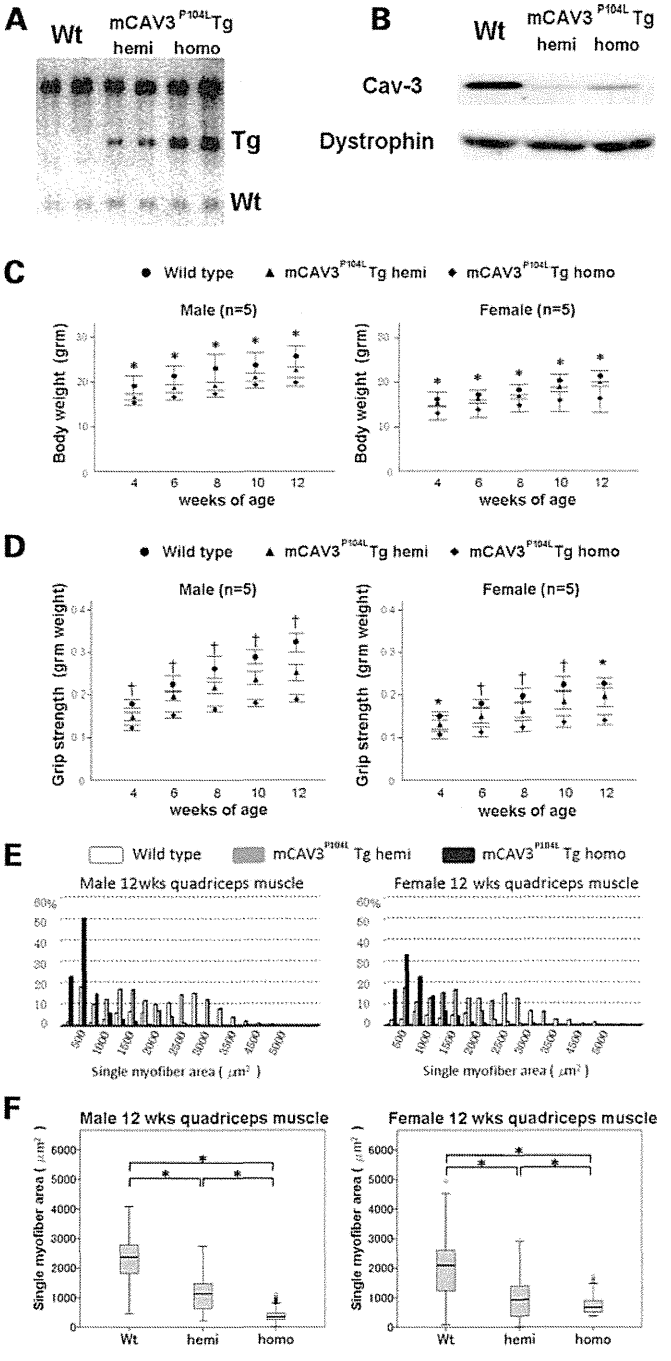

Figure 1. Effect of mCav3^{P104L} transgene dosage on the myopathic phenotype of LGMD1C model mice. (**A**) Genotyping of wild-type, hemizygous and homozygous transgenic mice by Southern blot analysis. A caveolin-3 DNA probe detected both endogenous caveolin-3 gene and mCav3^{P104L} transgene. Left to right, two independent samples of wild-type, hemizygous and homozygous transgenic mice. (**B**) Western blot analysis of caveolin-3 in skeletal muscles of wild-type and mCav3^{P104L} transgenic mice. Levels of caveolin-3 protein obviously decreased in the transgenic mice. Residual caveolin-3 was detected in homozygous mice. Temporal changes in body weight (**C**) and grip strength (**D**) of wild-type and transgenic mice between 4 and 12 weeks of age ($n = 5$ per group). Differences within each group were statistically determined using Scheffe's test. *Significant difference between wild-type and homozygous mice ($P < 0.05$). †Significant difference between each group ($P < 0.05$). Bars indicate standard error. (**E**) Histograms of individual myofiber areas in quadriceps muscle on transverse sections. Values were determined from 1000 myofibers per group. Bar = 100 μm. (**F**) Box plot represents non-parametric statistical analysis of myofiber areas of each group in (E). Significant difference between two groups (Mann–Whitney U test, *$P < 0.005$).

We immunohistochemically analyzed cleaved caspase-3 and cytochrome *c* to further elucidate the ER stress response toward apoptosis in myofibers. Caspase-3 is activated by proteolysis in the signaling cascade toward apoptosis (20). Cleaved caspase-3, which is an active form of caspase-3, is increased in response not only to ER stress but also to

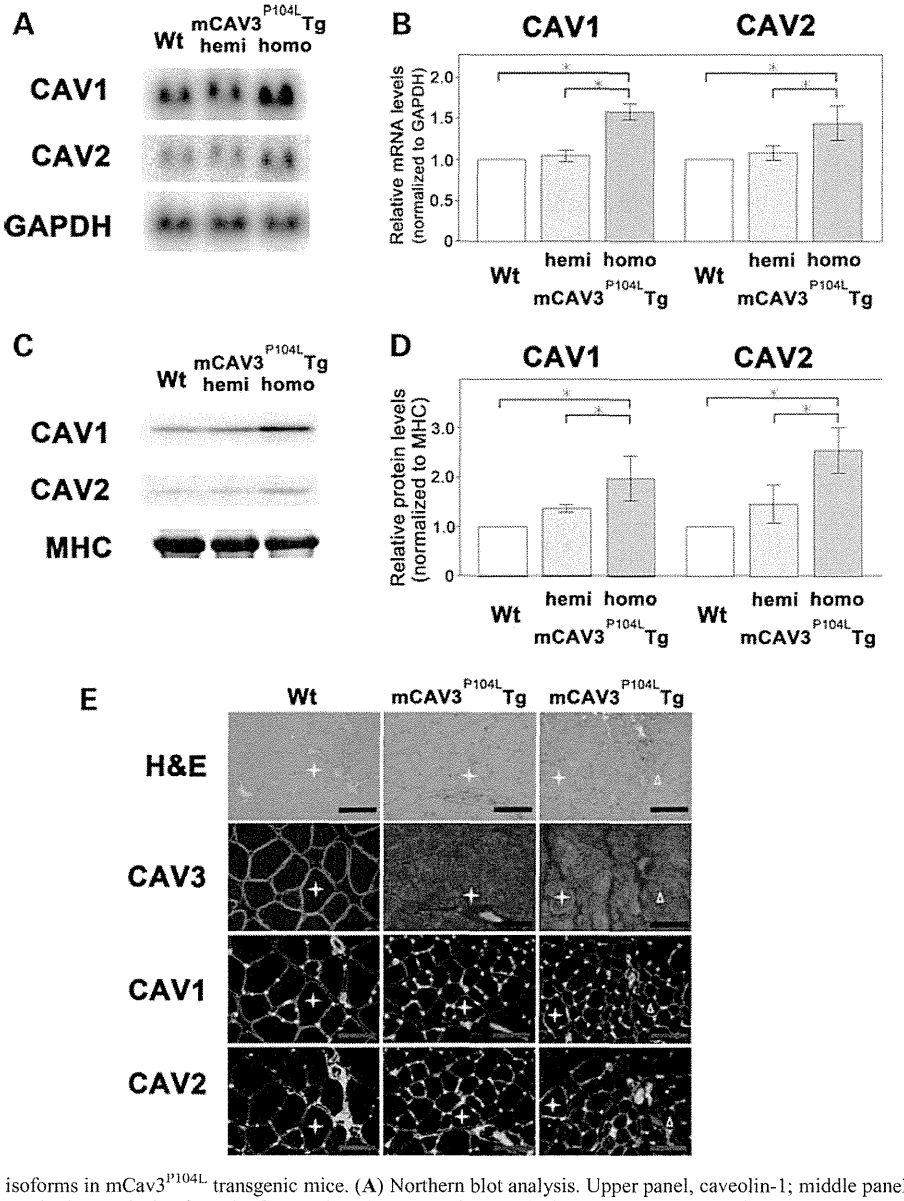

Figure 2. Expression of caveolin isoforms in mCav3^{P104L} transgenic mice. (**A**) Northern blot analysis. Upper panel, caveolin-1; middle panel, caveolin-2; lower panel, GAPDH as control. (**B**) Quantitative analysis of results from (A). (**C**) Western blot analysis. Upper panel, caveolin-1; middle panel, caveolin-2; lower panel, Coomassie blue-stained myosin heavy chain as standard control. (**D**) Quantitative analysis of results from (C). Signal intensity on blots determined from results of five independent experiments. Significant difference ($^*P < 0.05$) determined by Scheffe's test. (**E**) Immunohistochemical analysis of skeletal muscle cryosections from wild-type, hemizygous and homozygous transgenic mice. Crosses and triangles indicate identical myofibers on consecutive sections. H&E, hematoxylin and eosin staining. Caveolin isoforms, green; laminin, red.

apoptotic signals from the mitochondria (20,21). On the other hand, mitochondria specifically release cytochrome *c* into the cytosol under the latter conditions (20,22). Immunoreactivity for cleaved caspase-3 was obvious in the subsarcolemmal area of myofibers in mCav3^{P104L} transgenic mice (Fig. 5A). The average number of cleaved caspase-3 positive myofibers was increased in mCav3^{P104L} transgenic mice and differences between each genotype were significant (Fig. 5C). Cytochrome *c*-positive myofibers were rare in mCav3^{P104L} transgenic mice. Immunostained cleaved caspase-3 covered the entire area of myofibers that were frequently cytochrome *c*-positive in *mdx* and *dy*, but not in mCav3^{P104L} transgenic mice (Fig. 5A).

Apoptotic changes in myofibers were modest in mCav3^{P104L} transgenic mice compared with *mdx* or *dy* mice. We examined the expression of anti-apoptotic molecules from this perspective and found that *Dad1* mRNA was upregulated in mCav3^{P104L} transgenic mice (Fig. 6A and B). Dad1 is a subunit of the oligosaccharyl transferase complex that catalyzes the glycosylation of misfolded proteins to reduce ER stress (23,24). The upregulation of *Dad1* might contribute to the reduction of apoptosis in mCav3^{P104L} transgenic mice.

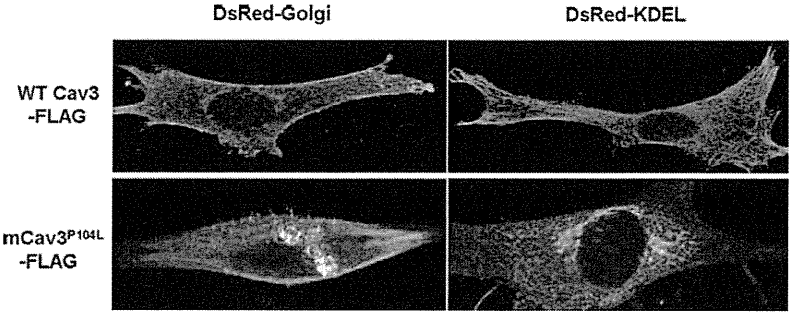

Figure 3. Immunostained C2C12 myoblasts transfected with wild-type or mCav3^{P104L} combined with a fluorescent marker that specifically localizes to ER or Golgi. Wild-type caveolin-3 (upper panels) and mCav3^{P104L} (lower panels) recognized by anti-FLAG tag antibody are shown in green. DsRed-Golgi marker (left panels) and DsRed-ER marker (right panels) recognized by anti-DsRed antibody are shown in red.

DISCUSSION

Mutations of the caveolin-3 gene cause LGMD with an autosomal dominant inheritance (6). Despite numerous studies *in vitro* using the disease-generating P104L mutant caveolin-3 (7–10), details of the molecular pathogenesis underlying LGMD1C have not been fully elucidated. Immunostaining for caveolin-3 at the sarcolemma is obviously lost in patients with LGMD1C (5,6). Galbiati's group proposed a dominant-negative effect of mutant caveolin-3 and demonstrated that it forms unstable aggregates of caveolin-3 hetero-oligomers with wild-type caveolin-3 that are retained in the Golgi complex (7) and that they are likely to be degraded by the ubiquitin–proteasome system (8). These data can explain why caveolin-3 protein levels were reduced in patients with LGMD1C. However, myopathy was notably milder in caveolin-3-null mice (25), but more severe in mCav3^{P104L} transgenic mice (13). Thus, a loss of caveolin-3 caused by the dominant-negative mechanism does not simply account for the severity of the disease in mice. A mechanism other than the reduced expression of caveolin-3 protein might function in the molecular pathogenesis of LGMD1C.

Here, we investigated phenotypic differences between hemizygous and homozygous mCAV3^{P104L} transgenic mice from morphological and molecular aspects. Myofiber hypotrophy and muscular weakness were more prominent in homozygous than in hemizygous mice. These findings indicated that the dosage of the mutant caveolin-3 transgene correlates with the severity of the myopathic phenotype. However, the lower level of residual caveolin-3 protein in hemizygous than in homozygous muscles is curious. This finding suggests that the level of mutant caveolin-3 determines the severity of myopathy through a toxic gain of function effect.

A unique feature of human LGMD1C is subsarcolemmal Golgi accumulation (possibly sarcoplasmic bodies) (5). The present and other studies have demonstrated mCav3^{P104L} accumulation in the Golgi apparatus *in vitro* (7,8,26). Previous pulse-chase experiments revealed that wild-type caveolin forms oligomers of about 400 kDa soon after the protein is synthesized in the ER (27). In addition, the mCav3^{P104L} proteins retained in the Golgi are composed of over 400 kDa high-molecular aggregates, and a proteasomal inhibitor causes such aggregates to accumulate within the ER (8). Together, newly synthesized mutant caveolin-3 protein could rapidly form misfolded aggregates in the ER, thereby inducing the ER stress response. Therefore, we analyzed the ER stress response to investigate a toxic gain of function effect of mCav3^{P104L}.

Indeed, we found that mCAV3^{P104L} induces the ER stress response in a gene-dose-dependent manner. Transcription of the molecular chaperone GRP78 was upregulated in mCav3^{P104L} transgenic mice. Under normal conditions, GRP78 suppresses the ER stress signaling pathway through direct interaction with ER stress transducers, such as PERK (16), which is a serine/threonine kinase that phosphorylates eIF2α (17,18). Misfolded proteins in the ER enlist GRP78 as a molecular chaperone. Once released from GRP78, the ER stress transducers trigger the cascade of gene regulation, known as the unfolded protein response (UPR). Molecular chaperones are commonly activated transcriptionally in the UPR (16). The phosphorylation of eIF2α by PERK is a crucial step in the UPR (17,18). We showed here that these molecular events occur in the skeletal muscle of mCav3^{P104L} transgenic mice, although PERK kinase activity was not directly demonstrated.

We also found that anti-apoptotic Dad1 (23,24) together with pro-apoptotic CHOP (18,19) is gene-dose dependently upregulated in mCAV3^{P104L} transgenic mice. This finding may be consistent with the limited numbers of TUNEL-positive myonuclei and cleaved caspase-3-positive myofibers in mCAV3^{P104L} transgenic mice compared with *mdx* or *dy* mice. Dystrophic changes such as necrotic/regenerating fibers or central nucleation are rarely observed and obvious myofiber hypotrophy is the most prominent feature of mCav3^{P104L} transgenic mice. Transgenic mice weigh less than wild-type mice by 4 weeks of age, which suggests the absence of normal hypertrophic growth or hypoplasia of the skeletal muscle. The most recent findings *in vitro* have revealed that the stable mCav3^{P104L} expression delays myoblast fusion (26). Therefore, the predominant small myofibers might be the result of impaired myotube formation rather than apoptosis. Overall, our results indicate that the apoptotic signaling in response to ER stress is counteracted by anti-apoptotic signaling in myofibers of mCav3^{P104L} transgenic mice, and that its contribution to myopathic change may be modest.

In conclusion, we demonstrated that mutant caveolin-3 dose-dependently induces the ER stress response, which would be a toxic gain of function effect related to the pathophysiology of LGMD1C.

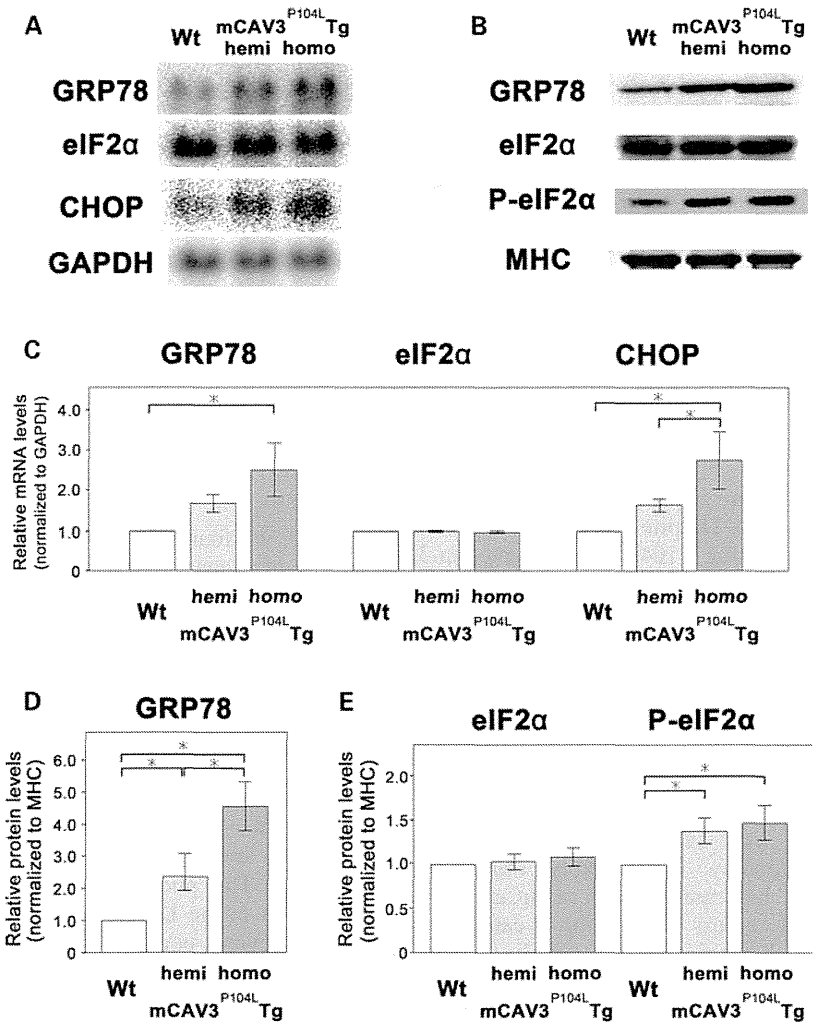

Figure 4. Endoplasmic reticulum stress response in mCav3^{P104L} transgenic mice. (**A**) Northern blot analysis of skeletal muscle from each group. Upper to lower panels, mRNA levels of GRP78, CHOP, eIF2α and GAPDH. (**B**) Western blot analysis of skeletal muscle from each group. Upper to lower panels, protein levels of GRP78, eIF2α and phosphorylated-eIF2α. Control Coomassie blue-stained myosin heavy chain. (**C**) Quantitative analysis of results from (A). (**D**) Quantitative analysis of GRP78 expression based on results from (B). Signal intensity on blots determined from results of five independent experiments. *Significant difference determined by Scheffe's test ($P < 0.05$).

MATERIALS AND METHODS

Animals

Mice were aged about 12 weeks in this study. The construct for the generation of mCav3^{P104L} transgenic mice has been described (13,14). All animal experiments proceeded at the Laboratory Animal Center under the approval of the Animal Research Committee of Kawasaki Medical School.

Muscle morphology and immunohistochemistry

Unfixed distal hindlimb muscles were snap-frozen in liquid nitrogen-cooled isopentane and sectioned transversely (10 μm) at the center of tibialis anterior (or quadriceps) muscle using a cryostat (Leica Microsystems). Sections were post-fixed in cold methanol for 10 min, and then immunostained using the Mouse on Mouse Kit (Vector Laboratories) according to the manufacturer's recommendations. The primary antibodies were as follows: rabbit polyclonal anti-caveolin-1 (BD Transduction Laboratories), mouse monoclonal anti-caveolin-2 (BD Transduction Laboratories), rabbit polyclonal anti-caveolin-3 (Alexis Corporation), rabbit polyclonal anti-cleaved caspase-3 (Cell Signaling Technology), anti cytochrome *c* (eBioscience) and rat monoclonal anti-laminin α2 (Alexis Corporation). Secondary antibodies were conjugated with fluorescein isothiocyanate.

Cell staining

C2C12 and COS7 cells were cultured on coverslips treated with the FuGENE6 transfection reagent (Roche) and then cotransfected with a caveolin-3-FLAG vector or an

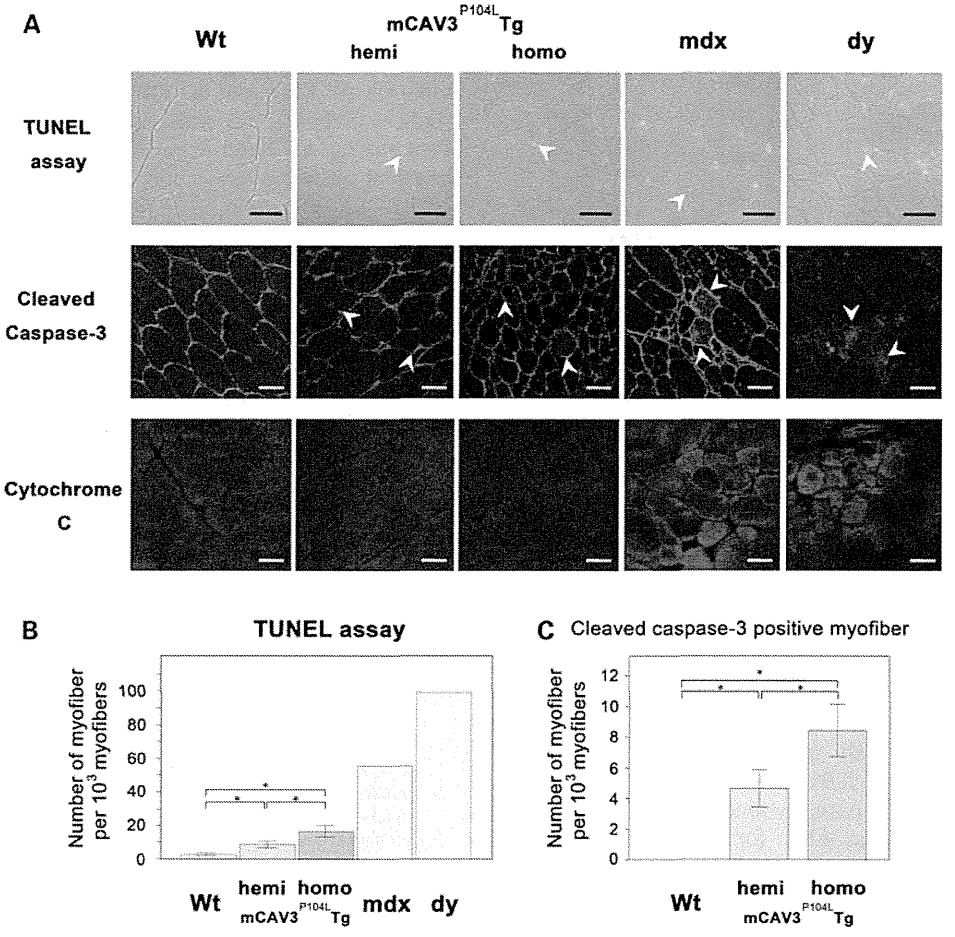

Figure 5. (**A**) (Upper panels) Typical appearance of apoptotic nuclei detected by TUNEL assays in mouse models of muscular dystrophy. Arrowheads indicate TUNEL-positive nuclei inside myofibers. (Middle and lower) Immunohistochemical analysis of skeletal muscle cryosections from mouse models of muscular dystrophy. (Middle panels) Cleaved caspase-3, red; laminin, green; DAPI, blue. Arrowheads indicate myofibers with immunoreactivity for cleaved caspase-3. (Lower panels) Cytochrome *c*, green. Bar = 50 μm (**B**) Numbers of myofibers with TUNEL-positive nuclei calculated per 1000 myofibers from independent samples ($n = 4$ per group of mutant caveolin-3 transgenic mice; positive control *mdx* and *dy* mice; $n = 2$ per group). Significant difference determined by Scheffe's test ($^*P < 0.05$). (**C**) Numbers of myofibers that were immunoreactive for cleaved caspase-3 per 1000 myofibers ($n = 3$ per group of mutant caveolin-3 transgenic mice). Significant difference determined by Scheffe's test ($^*P < 0.05$).

mCav3^{P104L} vector and pDsRed-Golgi (Clontech) or pCS2-DsRed-KDEL (a gift from Dr S. Nishimatsu). Twelve hours later, the cells were fixed in phosphate-buffered saline (PBS) containing 4% paraformaldehyde for 15 min and then permeabilized with PBS containing 0.5% Triton X-100 for 15 min. Non-specific binding was blocked with 3% bovine serum albumin in PBS containing 0.5% Triton X-100 for 1 h at room temperature. Cells were incubated with an anti-FLAG antibody (Sigma) and an anti-DsRed antibody (Clontech) at 4°C, followed by a secondary antibody.

TUNEL assay

Cryosections of quadriceps muscles (10 μm) were fixed with 1% paraformaldehyde in PBS for 10 min at room temperature. The sections were then post-fixed in ethanol:acetic acid (2:1) for 5 min at −20°C, labeled with digoxigenin-conjugated dNTP via the enzymatic activity of terminal deoxynucleotidyl transferase and reacted with anti-digoxigenin fluorescein antibody according to the manufacturer's recommendations (Chemicon). TUNEL-positive nuclei were counted in photographs of 15 sections from each sample.

RT-PCR

We reverse-transcribed cDNA templates from RNAs extracted from C2C12 cells. Genes were amplified using the following respective forward and reverse primers: caveolin-1, 5′-GACTGCCAAGCCTGTTGTAA-3′ and 5′-CAAACTGTG GCCATGCCAG-3′; caveolin-2, 5′-CATAAGGCTAGCTAG AGGCA-3′ and 5′-GGAGAGAACACCTAGACAGC-3′; GRP78, 5′CTTCGAAGGAGAAGACTTCTC-3′ and 5′-CTG TACCTTTGTCTTCAGCTG-3′; eIF2α, 5′-ATCTAATAGC TCCACCCAGG-3′ and 5′-AACAGCTGACATGA AGGAGG-3′; CHOP, 5′-CTGCCTTTCACCTTGGAGAC-3′ and 5′-GCTCGATTTCCTGCTTGAGC-3′; GAPDH, 5′-CGT AGACAAAATGGTGAAGG-3′ and 5′-GTTGTCATGGA TGACCTTGG-3′.

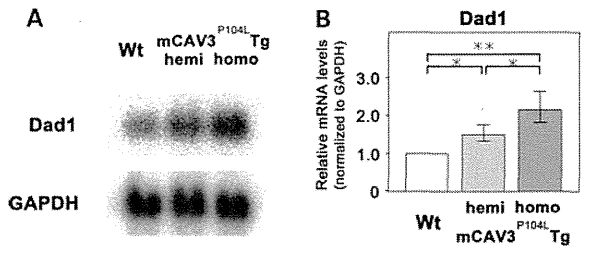

Figure 6. Upregulation of an anti-apoptotic molecule, Dad1, in mCav3^{P104L} transgenic mice. (**A**) Northern blot analysis of Dad1 in skeletal muscle from wild-type, hemizygous and homozygous transgenic mice. (**B**) Quantitative analysis of results from (A). Signal intensity on blots determined from results of five independent experiments. Significant difference determined by Scheffe's test ($^*P < 0.05$).

Northern blot analysis

The RT-PCR products of mouse cDNAs were subcloned into pCRII-TOPO (Invitrogen) and then digested with EcoRI. The digest was separated by agarose gel electrophoresis and extracted using the Rapid Gel Extraction System (Marligen Bioscience). Fragments of DNA were then labeled with [α-^{32}P]-dCTP using the MegaPrime DNA Labeling System (GE Healthcare) and RNAs were extracted from the skeletal muscles of mice in each genotype group. Total RNA (20 μg) was separated on 0.9% agarose gels containing 7% formaldehyde and blotted onto Hybond-N$^+$ (GE Healthcare). Hybridization proceeded at 42°C for 24 h, and then bands were visualized by autoradiography using Fuji Imaging Plates (Fujifilm). All northern blot experiments were repeated at least three times using different sets of samples.

Western blot analysis

Mouse skeletal muscles were homogenized in 10 volumes (w/v) of a buffer comprising 50 mM Tris–HCl (pH 7.4), 100 mM NaCl, 1 mM EDTA, 5 mM β-mercaptoethanol, 0.1 mM PMSF and 1 mM benzamidine. Crude muscle homogenates were separated by SDS-PAGE (3–20% linear acrylamide gradient) and transferred to polyvinylidene difluoride membranes. Antibodies were purchased from the indicated sources: goat polyclonal anti-GRP78 (Santa Cruz Biotechnology), mouse monoclonal anti-eIF2α (Abcam), rabbit polyclonal anti-Ser51 phosphorylated eIF2α (Abcam), rabbit polyclonal anti-caveolin-1 (BD Transduction Laboratories), mouse monoclonal anti-caveolin-2 (BD Transduction Laboratories) and rabbit polyclonal anti-caveolin-3 (Alexis Corporation). All western blot experiments were repeated at least five times, with different sets of samples. Immunoblot band intensities were standardized with Coomassie blue staining of myosin heavy chain in each sample and analyzed using Multi Gauge version 2.2 software (Fujifilm).

SUPPLEMENTARY MATERIAL

Supplementary Material is available at *HMG* online.

ACKNOWLEDGEMENTS

We thank M. Fujino (postgraduate student, Kawasaki Welfare School), A. Mimura, N. Oka and K. Yamane (Kawasaki Medical School), as well as N. Naoe and T. Kenmotsu (Department of Neurology, Kawasaki Medical School) for excellent technical assistance.

Conflict of Interest statement. None declared.

FUNDING

This study was supported by JSPS KAKENHI 20591013 and 21591101, a research grant for Nervous and Mental Disorders from the Ministry of Health, Labour and Welfare of Japan (20B-13), by grants for Research on Psychiatric and Neurological Diseases and Mental Health from the Ministry of Health, Labour and Welfare of Japan (H20-016, H20-018) and by research project grants from the Kawasaki Medical School (20-604, 21-602 and 22-T1).

REFERENCES

1. Richter, T., Floetenmeyer, M., Ferguson, C., Galea, J., Goh, J., Lindsay, M.R., Morgan, G.P., Marsh, B.J. and Parton, R.G. (2008) High-resolution 3D quantitative analysis of caveolar ultrastructure and caveola-cytoskeleton interactions. *Traffic*, **9**, 893–909.
2. Rothberg, K.G., Heuser, J.E., Donzell, W.C., Ying, Y., Glenney, J.R. and Anderson, R.G.W. (1992) Caveolin, a protein component of caveolae membrane coats. *Cell*, **68**, 673–682.
3. Song, K.S., Scherer, P.E., Tang, Z., Okamoto, T., Li, S., Chafel, M., Chu, C., Kohtz, D.S. and Lisanti, M.P. (1996) Expression of caveolin-3 in skeletal, cardiac, and smooth muscle cells. *J. Biol. Chem.*, **271**, 15160–15165.
4. Woodman, S.E., Sotgia, F., Galbiati, F., Minetti, C. and Lisanti, M.P. (2004) Caveolinopathies: mutations in caveolin-3 cause four distinct autosomal dominant muscle diseases. *Neurology*, **62**, 538–543.
5. Fulizio, L., Nascimbeni, A.C., Fanin, M., Piluso, G., Politano, L., Nigro, V. and Angelini, C. (2005) Molecular and muscle pathology in a series of caveolinopathy patients. *Hum. Mutat.*, **25**, 82–89.
6. Minetti, C., Sotgia, F., Bruno, C., Scartezzini, P., Broda, P., Bado, M., Masetti, E., Mazzocco, M., Egeo, A., Donati, M.A. *et al.* (1998) Mutations in the caveolin-3 gene cause autosomal dominant limb-girdle muscular dystrophy. *Nat. Genet.*, **18**, 365–368.
7. Galbiati, F., Volonté, D., Minetti, C., Chu, J.B. and Lisanti, M.P. (1999) Phenotypic behavior of caveolin-3 mutations that cause autosomal dominant limb girdle muscular dystrophy (LGMD-1C). *J. Biol. Chem.*, **274**, 25632–25641.
8. Galbiati, F., Volonté, D., Minetti, C., Bregman, D.B. and Lisanti, M.P. (2000) Limb-girdle muscular dystrophy (LGMD-1C) mutants of caveolin-3 undergo ubiquitination and proteasomal degradation. *J. Biol. Chem.*, **275**, 37702–37711.
9. Galbiati, F., Volonté, D., Engelman, J.A., Scherer, P.E. and Lisanti, M.P. (1999) Targeted down-regulation of caveolin-3 is sufficient to inhibit myotube formation in differentiating C2C12 myoblasts. *J. Biol. Chem.*, **274**, 30315–30321.
10. Fanzani, A., Stoppani, E., Gualandi, L., Giuliani, R., Galbiati, F., Rossi, S., Fra, A., Preti, A. and Marchesini, S. (2007) Phenotypic behavior of C2C12 myoblasts upon expression of the dystrophy-related caveolin-3 P104L and TFT mutants. *FEBS Lett.*, **581**, 5099–5104.
11. Conway, K.A., Harper, J.D. and Lansbury, P.T. (1998) Accelerated in vitro fibril formation by a mutant alpha-synuclein linked to early-onset Parkinson disease. *Nat. Med.*, **4**, 1318–1320.
12. Xiong, H., Wang, D., Chen, L., Choo, Y.S., Ma, H., Tang, C., Xia, K., Jiang, W., Ronai, Z., Zhuang, X. *et al.* (2009) Parkin, PINK1, and DJ-1 form a ubiquitin E3 ligase complex promoting unfolded protein degradation. *J. Clin. Invest.*, **119**, 650–660.

13. Sunada, Y., Ohi, H., Hase, A., Ohi, H., Hosono, T., Arata, S., Higuchi, S., Matsumura, K. and Shimizu, T. (2001) Transgenic mice expressing mutant caveolin-3 show severe myopathy associated with increased nNOS activity. *Hum. Mol. Genet.*, **10**, 173–178.
14. Ohsawa, Y., Toko, H., Katsura, M., Morimoto, K., Yamada, H., Ichikawa, Y., Murakami, T., Ohkuma, S., Komuro, I. and Sunada, Y. (2004) Overexpression of P104L mutant caveolin-3 in mice develops hypertrophic cardiomyopathy with enhanced contractility in association with increased endothelial nitric oxide synthase activity. *Hum. Mol. Genet.*, **13**, 151–157.
15. Ohsawa, Y., Hagiwara, H., Nakatani, M., Yasue, A., Moriyama, K., Murakami, T., Tsuchida, K., Noji, S. and Sunada, Y. (2006) Muscular atrophy of caveolin-3-deficient mice is rescued by myostatin inhibition. *J. Clin. Invest.*, **116**, 2924–2934.
16. Ni, M. and Lee, A.S. (2007) ER chaperones in mammalian development and human diseases. *FEBS Lett.*, **581**, 3641–3651.
17. Harding, H.P., Zhang, Y., Bertolotti, A., Zeng, H. and Ron, D. (2000) PERK is essential for translational regulation and cell survival during the unfolded protein response. *Mol. Cell*, **5**, 897–904.
18. Harding, H.P., Novoa, I., Zhang, Y., Zeng, H., Wek, R., Schapira, M. and Ron, D. (2000) Regulated translation initiation controls stress-induced gene expression in mammalian cells. *Mol. Cell*, **6**, 1099–1108.
19. Oyadomari, S. and Mori, M. (2004) Roles of CHOP/GADD153 in endoplasmic reticulum stress. *Cell Death Differ.*, **11**, 381–389.
20. Li, P., Nijhawan, D., Budihardjo, I., Srinivasula, S.M., Ahmad, M., Alnemri, E.S. and Wang, X. (1997) Cytochrome c and dATP-dependent formation of Apaf-1/caspase-9 complex initiates an apoptotic protease complex. *Cell*, **91**, 479–489.
21. Morishima, N., Nakanishi, K., Takenouchi, H., Shibata, T. and Yasuhiko, Y. (2002) An endoplasmic reticulum stress-specific caspase cascade in apoptosis. *J. Biol. Chem.*, **277**, 34287–34294.
22. Kluck, R.M., Bossy-Wetzel, E., Green, D.R. and Newmeyer, D.D. (1997) The release of cytochrome c from mitochondria. *Science*, **275**, 1132–1136.
23. Kelleher, D.J. and Gilmore, R. (1997) DAD1, the defender against apoptotic cell death, is a subunit of the mammalian oligosaccharyltransferase. *Proc. Natl. Acad. Sci. USA*, **94**, 4994–4999.
24. Kelleher, D.J. and Gilmore, R. (2006) An evolving view of the eukaryotic oligosaccharyltransferase. *Glycobiology*, **16**, 47R–62R.
25. Hagiwara, Y., Sasaoka, T., Araishi, K., Imamura, M., Yorifuji, H., Nonaka, I., Ozawa, E. and Kikuchi, T. (2000) Caveolin-3 deficiency causes muscle degeneration in mice. *Hum. Mol. Genet.*, **9**, 3047–3054.
26. Stoppani, E., Rossi, S., Meacci, E., Penna, F., Costelli, P., Bellucci, A., Faggi, F., Maiolo, D., Monti, E. and Fanzani, A. (2011) Point mutated caveolin-3 form (P104L) impairs myoblast differentiation via Akt and p38 signalling reduction, leading to an immature cell signature. *Biochim. Biophys. Acta*, **1812**, 468–479.
27. Monier, S., Parton, R.G., Vogel, F., Behlke, J., Henske, A. and Kurzchalia, T.V. (1995) VIP21-caveolin, a membrane protein constituent of the caveolar coat, oligomerizes in vivo and in vitro. *Mol. Biol. Cell*, **6**, 911–927.

THE JOURNAL OF BIOLOGICAL CHEMISTRY VOL. 287, NO. 12, pp. 9560–9567, March 16, 2012

Absence of Post-phosphoryl Modification in Dystroglycanopathy Mouse Models and Wild-type Tissues Expressing Non-laminin Binding Form of α-Dystroglycan*[S]

Received for publication, June 14, 2011, and in revised form, January 13, 2012 Published, JBC Papers in Press, January 23, 2012, DOI 10.1074/jbc.M111.271767

Atsushi Kuga[‡], Motoi Kanagawa[‡], Atsushi Sudo[‡], Yiumo Michael Chan[§], Michiko Tajiri[¶], Hiroshi Manya[‖], Yamato Kikkawa[**], Motoyoshi Nomizu[**], Kazuhiro Kobayashi[‡], Tamao Endo[‖], Qi L. Lu[§], Yoshinao Wada[¶], and Tatsushi Toda[‡1]

From the [‡]Division of Neurology/Molecular Brain Science, Kobe University Graduate School of Medicine, Kobe 650-0017, Japan, the [§]McColl-Lockwood Laboratory for Muscular Dystrophy Research, Neuromuscular/ALS Center, Carolinas Medical Center, Charlotte, North Carolina 28231, the [¶]Department of Molecular Medicine, Osaka Medical Center and Research Institute for Maternal and Child Health, Osaka 594-1101, Japan, [‖]Molecular Glycobiology, Tokyo Metropolitan Institute of Gerontology, Tokyo 173-0015, Japan, and the [**]Laboratory of Clinical Biochemistry, School of Pharmacy, Tokyo University of Pharmacy and Life Sciences, Tokyo 192-0392, Japan

Background: The biosynthetic pathway for the ligand-binding moiety of α-dystroglycan, defects in which cause dystroglycanopathy, remains unclear.
Results: The phosphodiester-linked moiety on *O*-mannose is absent in dystroglycanopathy models and in wild-type lung and testis.
Conclusion: Post-phosphoryl modification is a key determinant of the functional expression of α-dystroglycan as a laminin receptor.
Significance: This work expands our understanding of the molecular mechanism of a unique post-translational modification.

α-Dystroglycan (α-DG) is a membrane-associated glycoprotein that interacts with several extracellular matrix proteins, including laminin and agrin. Aberrant glycosylation of α-DG disrupts its interaction with ligands and causes a certain type of muscular dystrophy commonly referred to as dystroglycanopathy. It has been reported that a unique *O*-mannosyl tetrasaccharide (Neu5Ac-α2,3-Gal-β1,4-GlcNAc-β1,2-Man) and a phosphodiester-linked modification on *O*-mannose play important roles in the laminin binding activity of α-DG. In this study, we use several dystroglycanopathy mouse models to demonstrate that, in addition to fukutin and LARGE, FKRP (fukutin-related protein) is also involved in the post-phosphoryl modification of *O*-mannose on α-DG. Furthermore, we have found that the glycosylation status of α-DG in lung and testis is minimally affected by defects in *fukutin*, *LARGE*, or *FKRP*. α-DG prepared from wild-type lung- or testis-derived cells lacks the post-phosphoryl moiety and shows little laminin-binding activity. These results show that FKRP is involved in post-phosphoryl modification rather than in *O*-mannosyl tetrasaccharide synthesis. Our data also demonstrate that post-phosphoryl modification not only plays critical roles in the pathogenesis of dystroglycanopathy but also is a key determinant of α-DG functional expression as a laminin receptor in normal tissues and cells.

Dystroglycan (DG),[2] a cell surface receptor for several extracellular matrix proteins, plays important roles in various tissues (1). DG consists of a heavily glycosylated extracellular α subunit (α-DG) and a transmembrane β subunit (β-DG). α-DG and β-DG are encoded by a single gene and post-translationally cleaved to generate the two subunits (2). α-DG binds to extracellular proteins such as laminin, agrin, perlecan, neurexin, and pikachurin (2–7). β-DG anchors α-DG at the cell surface and binds intracellularly to dystrophin, which in turn binds to the actin cytoskeleton. Thus, α/β-DG functions as a molecular axis, connecting the extracellular matrix with the cytoskeleton across the plasma membrane (1).

O-Glycosylation of α-DG is necessary for its interaction with ligands, and genetic disruption of the glycosylation pathway for DG is associated with a group of muscular dystrophies known as "dystroglycanopathy" (8–10). Six genes (*POMT1*, *POMT2*, *POMGnT1*, *fukutin*, *FKRP*, and *LARGE*) have been identified as causative genes for dystroglycanopathy. A common biochemical characteristic of these disorders is abnormal glycosylation and reduced laminin-binding activity of α-DG; however, the precise glycan structure required for α-DG ligand binding is not completely determined. Two unique *O*-mannosyl modifications have been identified in α-DG: an *O*-mannosyl tetrasaccharide (Neu5Ac-α2,3-Gal-β1,4-GlcNAc-β1,2-Man) (11), and

* This work was supported by Ministry of Health, Labor, and Welfare of Japan Intramural Research Grant (23B-5) for Neurological and Mental Disorders and The Research on Psychiatric and Neurological Diseases and Mental Health H20-016 (to T. T.), Grant-in-aid for Scientific Research (A) 23249049 (to T. T.) and a Grant-in-aid for Young Scientists (B) 21790318 (to M. K.) from the Ministry of Education, Culture, Sports, Science, and Technology of Japan, and the Takeda Science Foundation (to M. K.).
[S] This article contains supplemental Fig. 1.
[1] To whom correspondence should be addressed: 7-5-1 Kusunoki-chou Chuo-ku, Kobe 650-0017, Japan. Tel.: 81-78-382-6287; Fax: 81-78-382-6288; E-mail : toda@med.kobe-u.ac.jp.

[2] The abbreviations used are: DG, dystroglycan; IMAC, immobilized metal affinity chromatography; MW, molecular weight; HFaq, aqueous hydrofluoric acid.

a phosphodiester-linked branch structure present at the C6 hydroxyl residue of *O*-mannose (12). The *O*-mannosyl tetrasaccharide was first identified on peripheral nerve α-DG (11). The initial mannose transferred to Ser/Thr residues on the α-DG polypeptide backbone is catalyzed by the POMT1/POMT2 complex (13). Mutations in *POMT1* and *POMT2* were originally identified as causative for Walker-Warburg syndrome (14, 15). *POMGnT1*, established as a causative gene for muscle-eye-brain disease, encodes a glycosyltransferase that transfers GlcNAc to *O*-mannose on α-DG (16). In these disorders, α-DG lacks laminin-binding activity (17); therefore, the tetrasaccharide plays an important role in the post-translational maturation of α-DG as a laminin receptor. On the other hand, recent studies have suggested that the Neu5Ac-α2,3-Gal-β1,4-GlcNAc branch on *O*-mannose *per se* is not likely the laminin-binding glycan of α-DG (12, 18).

fukutin was originally identified as the causative gene for Fukuyama-type congenital muscular dystrophy (19), and *FKRP* was identified as the causative gene for both MDC1C (congenital muscular dystrophy type 1C) (20) and LGMD2I (limb-girdle muscular dystrophy type 2I) (21). The precise function of fukutin and FKRP is still uncertain. Mutation of *LARGE* causes muscular dystrophy in the spontaneous *Large*^{myd} mouse model (22) and in human congenital muscular dystrophy type 1D (23). Recently, a phosphodiester-linked modification on an *O*-mannose was identified (12). It was shown that α-DG in *fukutin*-mutated Fukuyama-type congenital muscular dystrophy and *Large*^{myd} muscle cells exhibits defective post-phosphoryl modification on the *O*-mannose, suggesting that this phosphorylated branch serves as the laminin-binding moiety. To explore the role of phosphorylated *O*-mannose in functional α-DG ligand-binding and in other forms of dystroglycanopathy, we have investigated α-DG glycosylation in several dystroglycanopathy mouse models.

EXPERIMENTAL PROCEDURES

Cell Culture—TM3 and CHL cell lines were purchased from European collection of cell cultures and the RIKEN BioResource Center, respectively. TM3 cells were cultured in Ham's F12/DMEM (1:1) containing 5% horse serum and 2.5% fetal bovine serum. CHL cells were cultured in DMEM containing 10% fetal bovine serum. Expression vectors for LARGE were constructed by cloning human *LARGE* with a V5 tag into pcDNA vectors (24). Transfection was carried out using Lipofectamine 2000 (Invitrogen) for CHL and TM3 cells according to the manufacturer's instructions. Transfected cells were grown at 37 °C and harvested at 48 h after transfection. The transfected cells were solubilized in TBS with 1% Triton X-100. Samples were centrifuged at 15,000 rpm for 10 min at 4 °C. Supernatants were collected, and protein concentrations were measured by Lowry methods, using BSA as a standard.

Animals—*Large*^{myd} mice were obtained from The Jackson Laboratory. Generation of FKRP-neo-P448L knock-in mice, Hp/− mice, and *POMGnT1*-deficient mice has been described previously (25–27). Mice were maintained in accordance with the animal care guidelines of Kobe University. All animal studies using FKRP-neo-P448L knock-in mice were approved by the Institutional Animal Care and Use Committee of the Carolinas Medical Center.

Protein Enrichment—Frozen tissue samples were solubilized in TBS (pH 7.4) with 1% Triton X-100. The solubilized materials were incubated with wheat germ agglutinin beads, and the DG-enriched fraction was then eluted with 0.3 M *N*-acetyl-D-glucosamine in TBS containing 0.1% Triton X-100. For the immobilized metal affinity chromatography (IMAC)-binding assay, aqueous hydrofluoric acid (HFaq) treatment, and deglycosylation assay, the DG-enriched fractions were diluted in 0.25% CHAPS/water (w/v) and then desalted and concentrated using Amicon-ultra filters (Millipore).

IMAC-binding Assay—Samples were diluted in a solution containing 250 mM acetic acid, 30% acetonitrile, and 0.15% CHAPS and incubated with PHOS-Select iron affinity gel (Sigma) at room temperature for 0.5 h. Bound materials were directly eluted with SDS-loading buffer. Equal ratios of the void and the bound samples were used for Western blot analysis.

HFaq Treatment—Samples were incubated with 48% aqueous hydrofluoric acid (Wako) on ice for 12 h. Control samples were incubated with water instead of hydrofluoric acid. After removal of the reagents under a stream of nitrogen gas, residues were dissolved with SDS-loading buffer for Western blot analysis.

Deglycosylation Assay—Glycopeptidase F (peptide-*N*-glycosidase; Wako), α-2 (3, 6, 8, 9) neuraminidase (Calbiochem), β1–4 galactosidase (New England Biolabs), β-*N*-acetyl-hexosaminidase (Seikagaku Corp.), and *O*-glycosidase (Roche Applied Science) were used according to the manufacturer's protocol.

Antibodies—Antibodies used for Western blotting were mouse monoclonal antibody IIH6 against glycosylated α-DG (Millipore) and goat polyclonal antibody against the C-terminal domain of the α-DG polypeptide (AP-074G-C) (26).

Laminin and Agrin Overlay Assays—Recombinant mouse laminin LG4–5 domains of laminin α1 and laminin α2 chains fused to Fc tags were recovered from the cell culture media using protein A beads (28). Recombinant agrin was purchased from R&D Systems. Laminin and agrin overlay assays were performed as described previously (26).

RT-PCR Analysis—Total RNA was isolated from wild-type mouse testis and TM3 cells using the RNeasy Plus mini kit (Qiagen) and converted to cDNA using Superscript III reverse transcriptase (Invitrogen). The forward and reverse primers used in gene amplification were as follows: *Large* (5′-TCAATCTTCTGCGAAACGTG-3′ and 5′-TCCAACATTGACAGCAGCTC-3′), *POMT1* (5′-CGGGTCTCTTGTTCCTGTG-3′ and 5′-AGTGACTGAGCACGCGCATA-3′), *POMT2* (5′-CGGAACCTGCACAGTCACTA-3′ and 5′-AATCCGCCAGAAGTCATTTG-3′), *POMGnT1* (5′-CCAAGGGGTATCTCCACAGA-3′ and 5′-GGTCCTCTTCCAGAACCACA-3′), *fukutin* (5′-CGCACTGCAGTATCACCTGT-3′ and 5′-AAGTGGATGGCATGAGTGGT-3′), *FKRP* (5′-CTTCTGTCCCGCTTCAGTTC-3′ and 5′-AACCAGAGAGAGCCCAGTCA-3′), *β3GnT1* (5′-TTCAATCGAATCAGCCAGGTA-3′ and 5′-TCCTCAATTCTCCATCATCCA-3′), GAPDH (5′-CGTAGACAAAATGGTGAAGG-3′ and 5′-GTTGTCATGGAT-

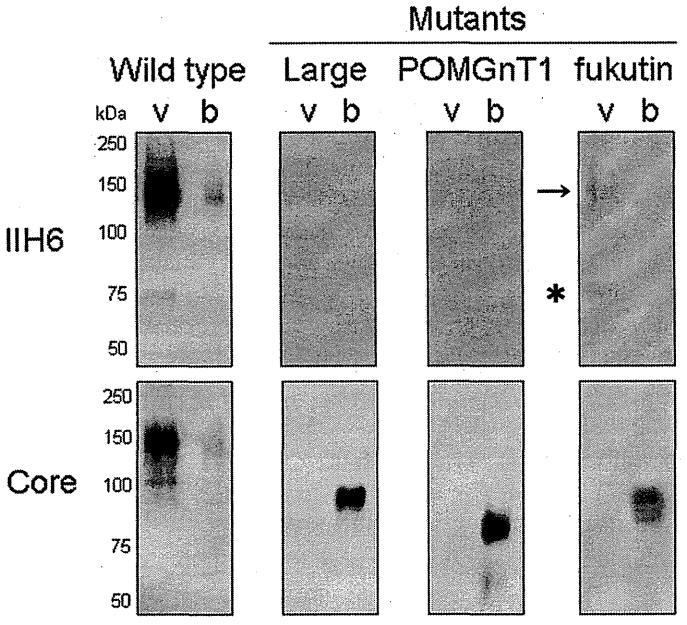

FIGURE 1. **Defects of post-phosphoryl modification in the dystroglycanopathy models.** α-DG-enriched samples from skeletal muscle of wild-type, *Large*^{myd}, *POMGnT1*-deficient, and *fukutin*-deficient Hp/− mice were subjected to IMAC beads. The void (*v*) and bound (*b*) fractions were collected. An *arrow* indicates the IIH6-positive intact α-DG in the Hp/− mice. An *asterisk* indicates a background signal that is not specific for IIH6 antibody.

GACCTTGG-3′), and *DAG1* (5′-ACCAAAGCACCCATCACCAG-3′ and 5′-GTTCCCACCCAGGCATCTAC-3′).

RESULTS

Defects of Post-phosphoryl Modification in FKRP-deficient Mice—To examine whether dystroglycanopathy models share a common defect in the post-phosphoryl modification of α-DG, we performed an IMAC bead-binding assay. IMAC beads bind to monoester-linked, but not diester-linked, phosphorylated compounds, and it has been shown that α-DG with defects in post-phosphoryl modification binds to IMAC beads (12). First, we used *Large*^{myd} mice (22), genetically engineered *POMGnT1* knock-out mice (27), and transgenic Hp/− knock-in mice carrying the retrotransposal insertion in *fukutin* (26). α-DG in skeletal muscle tissues from these mutant mice was not properly glycosylated, as indicated by the loss of reactivity against the monoclonal antibody IIH6 (Fig. 1, *upper panel*). The hypoglycosylated α-DG has a lower molecular weight (MW) that can only be detected by the DG core antibody (Fig. 1, *lower panel*). IIH6 antibody reacts with the laminin-binding glycans present in α-DG (17). Hypoglycosylated α-DG was captured by the IMAC beads, indicating that the monoester-linked phosphate residues do not undergo further modification. A small portion of α-DG with a MW of 150,000 in the Hp/− mice (Fig. 1, *arrow*) did not bind to the IMAC beads and showed reactivity against the IIH6 antibody, which might be due to the residual activity of fukutin in the Hp/− mice (26). These data support the observations made in muscle-eye-brain disease and Fukuyama-type congenital muscular dystrophy patients' cells and skeletal muscle biopsies (12).

We next examined whether FKRP is also involved in the post-phosphoryl modification of α-DG. Consistent with previous observations, α-DG from the skeletal muscle of homozygous FKRP-neo-P448L knock-in mice (FKRP-P448L mice) was aberrantly glycosylated, as indicated by the loss of IIH6 reactivity (25). The hypoglycosylated α-DG, showing a lower MW of 90,000 compared with wild-type α-DG at 150,000, bound to the IMAC beads (Fig. 2*A*, *lower panel*). In brain tissue, IIH6-positive α-DG shows a MW of 100,000, whereas hypoglycosylated α-DG shows a MW of 70,000. As was the case in skeletal muscle, hypoglycosylated α-DG from the homozygous mouse bound to IMAC beads (Fig. 2*A*). It has been reported that treatment with cold HFaq cleaves the phosphodiester linker in α-DG (12). After HFaq treatment, the MW of α-DG was reduced to ~90,000, and α-DG lost IIH6-reactivity (Fig. 2*B*, *left panel*). In contrast to the mature α-DG from heterozygous controls, the hypoglycosylated α-DG from homozygous FKRP-P448L muscle showed almost no change in MW after the HFaq treatment (Fig. 2*B*, *right panel*). Treatment with several mixtures of glycosidase predicted to remove *N*-glycan, mucin type *O*-glycan, and the trisaccharide at the non-reducing end of the Neu5Ac-α2,3-Gal-β1,4-GlcNAc-β1,2-Man glycan (12, 18) generated stepwise decreases in the MW of α-DG through multi-step digestions (Fig. 2*C*). These results indicate for the first time that FKRP is involved in the post-phosphoryl modification of α-DG rather than in the synthesis of the Neu5Ac-α2,3-Gal-β1,4-GlcNAc-β1,2-Man glycan. This concept is supported by the previous observation that neither POMT1/2 nor POMGnT1 activity was reduced in lymphoblast cells from patients with *FKRP* mutations (29). Overall, our results establish and confirm that a defect in post-phosphoryl modification on *O*-mannose is a common biochemical characteristic in dystroglycanopathy caused by mutations in *LARGE*, *POMGnT1*, *fukutin*, and *FKRP*.

Post-phosphoryl Moiety of α-dystroglycan Is Absent in Lung and Testis—We have demonstrated that disruption of *Large*, *fukutin*, or *FKRP* decreases the MW of α-DG in skeletal muscle and brain due to the lack of post-phosphoryl modification. It is known that the MW of α-DG and its reactivity to the monoclonal antibody IIH6 vary among different tissues (1, 30). We hypothesized that the low MW of α-DG in some tissues may result from the lack of post-phosphoryl modification and/or the Neu5Ac-α2,3-Gal-β1,4-GlcNAc-β1,2-Man glycan. Several tissues from dystroglycanopathy model mice were therefore investigated. We found that the decreases in the MW of α-DG were relatively minor in lung and very scarce in testis from FKRP-P448L mice and Hp/− mice when compared with litter controls (Fig. 3*A*). Minor changes in α-DG MW in the lung and testis of *Large*-deficient mice have been also observed elsewhere (30), supporting our findings. On the other hand, α-DG in lung and testis from *POMGnT1*-deficient mice clearly shows a lower MW compared with litter heterozygous controls and other mutant mouse strains (Fig. 3*B*). These results suggested that the GlcNAc-β1,2 branch on *O*-mannose is present in wild-type α-DG in lung and testis, but post-phosphoryl modification is absent.

We examined these tissues in wild-type mice using an IMAC bead-binding assay and HFaq treatment. In Fig. 4*A*, Western blot analysis of wild-type tissues showed that α-DG in testis has a MW of 90,000 and was not recognized by the IIH6 antibody,

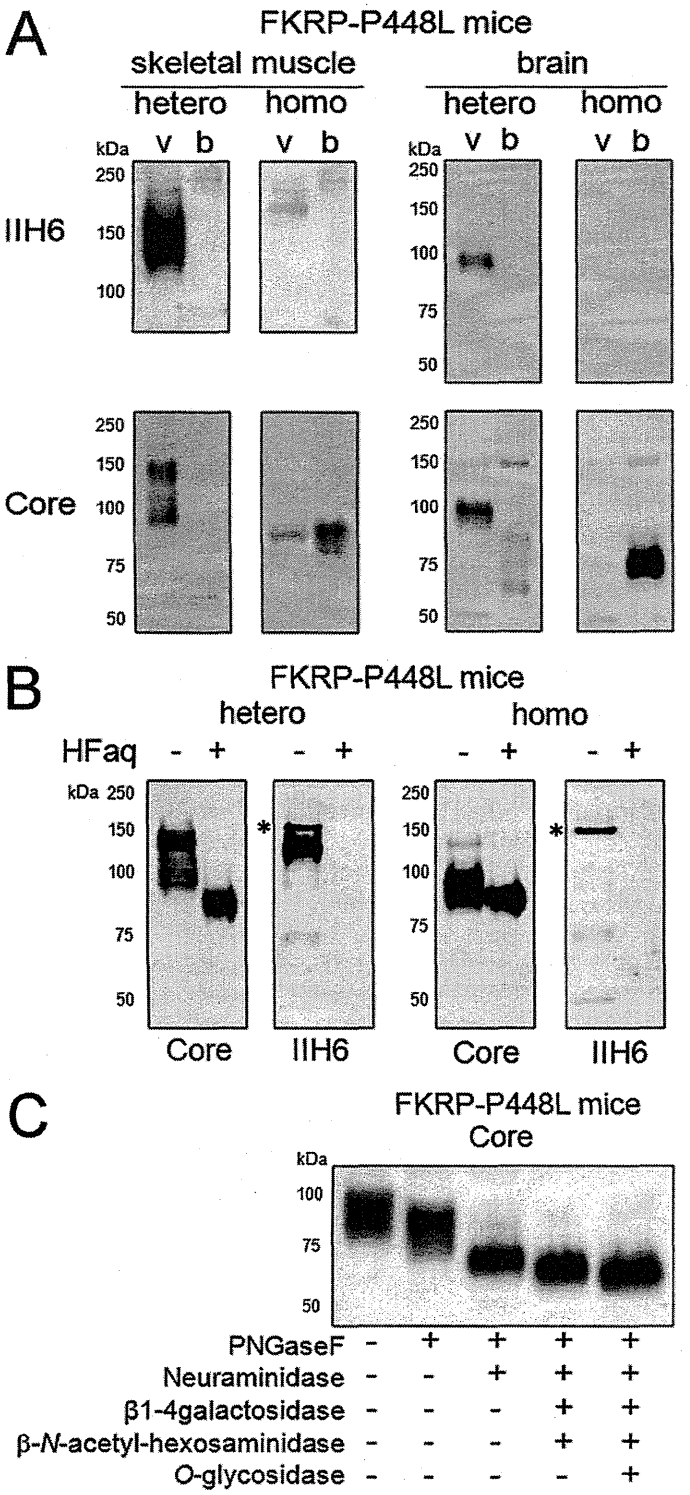

FIGURE 2. **Defects of post-phosphoryl modification in the *FKRP*-deficient disease model.** *A*, IMAC bead-binding assay for *FKRP*-deficient mice. α-DG enriched samples from skeletal muscle and brain of FKRP-P448L homozygous (*homo*) and litter control heterozygous (*hetero*) mice were tested for binding to IMAC beads. The void (v) and bound (b) fractions were collected. *B*, chemical dephosphorylation of α-DG from *FKRP*-deficient mice. α-DG enriched samples from skeletal muscle of FKRP-P448L homozygous (*homo*) and litter control heterozygous (*hetero*) mice were treated with HFaq. *, these bands are not likely derived from α-DG because they are not recognized by antibodies against the α-DG core protein. *C*, enzymatic deglycosylation of α-DG from *FKRP*-deficient mice. α-DG-enriched samples from skeletal muscle of FKRP-P448L homozygous mice were digested with glycosidase mixtures (peptide-*N*-glycosidase (*PNGase F*), neuraminidase, β1–4 galactosidase/β-*N*-acetyl-hexosaminidase, and *O*-glycosidase). Following the IMAC bead-binding assay, HFaq treatment, and enzymatic digestions, the samples were analyzed by Western blot, using antibodies against the α-DG core protein (*Core*) or the functionally glycosylated form (*IIH6*). *v*, void fraction; *b*, bound fraction.

and that lung α-DG consists of two major detectable populations (IIH6-positive > 100,000, minor form, *arrow*; IIH6-negative < 100,000, major form, *arrowhead*). Both testis and lung IIH6-negative α-DG were found to bind to IMAC beads, in contrast with IIH6-positive α-DG in skeletal muscle, brain, liver, and lung (Fig. 4*A*). Furthermore, HFaq treatment reduced the MW of α-DG to ~75,000 in wild-type skeletal muscle, brain, and liver. On the other hand, the MW shift observed in testis α-DG and IIH6-negative lung α-DG was relatively minor following HFaq treatment (Fig. 4*B*). These data indicate the absence of post-phosphoryl modification on α-DG in some wild-type tissues. Ligand overlay assays showed that IIH6-positive α-DGs in skeletal muscle, brain, and lung bound to the ligand proteins laminin α1, α2, and agrin, whereas IIH6-negative α-DG in testis and lung did not bind to these ligands (Fig. 5). Altogether, these data confirm that IIH6-reactivity and laminin-binding activity in α-DG are associated with post-phosphoryl modification.

Because lung and testis tissues contain heterogeneous cell types, we also examined the established cell lines CHL (lung epithelial cells derived from Chinese hamster) and TM3 (Leydig cells derived from mouse testis). Both CHL and TM3 cells showed detectable amounts of endogenous α-DG using the core antibody, but they did not react with IIH6 (Fig. 6, *A* and *D*). RT-PCR analysis showed that known genes (*Large*, *POMT1*, *POMT2*, *POMGnT1*, *fukutin*, *FKRP*, and *β3GnT1*) involved in α-DG glycosylation were expressed in TM3 cells (Fig. 6*B*). β3GnT1 has been reported to be required for laminin-binding glycan synthesis through formation of a complex with LARGE (31). We did not examine expression in CHL cells because the sequences of these genes have not yet been determined in the hamster. Endogenous α-DG in CHL and TM3 cells bound to IMAC beads (Fig. 6*A*). HFaq treatment resulted in almost no change in the MW of α-DG in both CHL and TM3 cells (Fig. 6*C*), as was similarly seen in lung and testis tissues (Fig. 4*B*). Following sequential digestion with glycosidases, α-DG in both CHL and TM3 cells showed stepwise reductions in MW (Fig. 6*D*). These data suggest that the post-phosphoryl modification is absent from IIH6-negative α-DG in CHL and TM3 cells.

DISCUSSION

In the present study, we demonstrate for the first time that FKRP is involved in post-phosphoryl modification on *O*-mannose of α-DG. We also show that even in wild type, α-DG in certain tissues such as lung and testis lacks the post-phosphoryl modification.

Abnormal glycosylation of α-DG in dystroglycanopathies is usually determined by a loss of reactivity against monoclonal antibodies VIA4–1 or IIH6. Mutations in the POMT1/POMT2 complex result in *O*-mannosylation defects (13–15); therefore, *O*-mannosyl phosphorylation does not occur. α-DG in cells with mutations in *Large*, *fukutin*, or *POMGnT1* does not undergo further modification from phospho-mannose residues